JOURNAL OF GEOPHYSICAL RESEARCH, VOL. 107, NO. E5, 5028, 10.1029/2000JE001458, 2002

# Morphology of Europan bands at high resolution: A mid-ocean ridge-type rift mechanism

Louise M. Prockter,[1,2] James W. Head III,[1] Robert T. Pappalardo,[1] Robert J. Sullivan,[3] Amy E. Clifton,[4] Bernd Giese,[5] Roland Wagner,[5] and Gerhard Neukum[5]

Received 26 January 2001; revised 30 August 2001; accepted 2 October 2001; published 14 May 2002.

[1] We utilize imaging data from the Galileo spacecraft to investigate band formation on one of Jupiter's moons, Europa. Bands are polygonal features first observed in Voyager data close to Europa's anti-Jovian point and represent areas where preexisting terrain has been pulled apart, allowing new material to move up into the gap. We examine the detailed morphology of several bands imaged at different resolutions and lighting geometries. We identify several distinct morphological characteristics, including central troughs, hummocky textures, and ridge and trough terrains, some of which are common among the bands studied. In many cases, bands have initiated along segments of one or more preexisting double ridges, ubiquitous within Europa's ridged plains. Distinctive morphological features and high standing topography imply that the bands formed from compositionally or thermally buoyant ice, rather than liquid water. Comparisons between Europan band morphologies and features found on terrestrial mid-ocean ridges reveal several similarities, including axial troughs, subcircular hummocks, normal faults, and indications of symmetrical spreading. We conclude that terrestrial mid-ocean ridge rifting is a good analogy for Europan band formation. If a terrestrial seafloor-spreading model is applicable to Europan bands, we speculate that band morphologies might be related to the relative rate of spreading of each band. Bands may have contributed significantly to the resurfacing of Europa. Europan bands we examine predate (but do not postdate) lenticulae and related features, implying that the style of resurfacing on Europa has changed over recent geological time in these regions. *INDEX TERMS:* 5475 Planetology: Solid Surface Planets: Tectonics (8149); 3035 Marine Geology and Geophysics: Midocean ridge processes; 3045 Marine Geology and Geophysics: Seafloor morphology and bottom photography; 6218 Planetology: Solar System Objects: Jovian satellites; *KEYWORDS:* Europa, mid-ocean ridge, rift, gray band, Galileo, morphology

## 1. Introduction

[2] The Galileo spacecraft has been in orbit around Jupiter since 1995, imaging its four largest moons. The second of these from Jupiter, Europa, is a largely silicate body with an outermost 100 km layer composed primarily of water and/or ice [*Anderson et al.*, 1998]. A vast region of dark linear and wedge-shaped bands $\leq$25 km wide and up to several hundred kilometers long was observed near Europa's anti-Jovian tidal bulge by Voyager at 2 km/pixel (Figure 1) [*Smith et al.*, 1979; *Schenk and McKinnon*, 1989]. Using Voyager image data, *Schenk and McKinnon* [1989] noted that the dark material of some of these features could be removed, allowing the margins of the bands to fit closely together and the surrounding preexisting lineaments to be reconstructed. They interpreted fracturing to have occurred in a brittle lithosphere overlying a deformable material; thus the presence of these ''pull-apart'' bands indicates that complete opening of the lithosphere has occurred, with low-albedo material filling in the newly created gap. *Pappalardo and Sullivan* [1996] successfully performed the same type of reconstruction on the gray band Thynia Linea located to the south of the anti-Jovian tidal bulge, and *Tufts et al.* [1999] reconstructed the southern hemisphere strike-slip fault Astypalaea Linea in a similar manner. The successful restoration of preexisting features on either side of the bands implies that failure was along near-vertical tension fractures, rather than along normal faults forming graben. As a result, *Golombek and Banerdt* [1990] inferred a $\sim$6 km upper limit for Europa's lithospheric thickness at the time of deformation.

[3] Galileo imaging at regional resolutions (hundreds of meters per pixel) showed that many dark bands could be reconstructed perfectly, confirming that complete lithospheric separation had occurred [*Tufts et al.*, 1997, 2000; *Sullivan et al.*, 1998]. Parallel linear structures observed within the bands appear to be approximately ''mirrored'' on either side of the central axis of the band, implying that bands open broadly symmetrically along a central axis [*Sullivan et al.*, 1998]. *Schenk and McKinnon* [1989] and *Sullivan et al.* [1998] suggested that the type of rifting observed on Europa could be analogous to that seen on the Earth at mid-ocean ridges, where crustal plates are pulled apart and new lithospheric material is brought up to the surface to fill the gaps. As was noted by *Schenk and McKinnon* [1989], Europa is the only place in the solar system other than Earth where complete separation of the lithosphere such as this is inferred to have occurred. Therefore the study of terrestrial mid-ocean ridges can aid in the interpretation of Europa's bands. Conversely, as the only other known locale of lithospheric separation, Europa may provide insight into the variety

[1]Department of Geological Sciences, Brown University, Providence, Rhode Island, USA.
[2]Now at Applied Physics Laboratory, Laurel, Maryland, USA.
[3]Center for Radiophysics and Space Research, Cornell University, Ithaca, New York, USA.
[4]Nordic Volcanological Institute, Reykjavik, Iceland.
[5]Institute of Planetary Exploration, DLR, Berlin, Germany.


0148-0227/02/2000JE001458

**Figure 1.** Galileo Global mosaic of Europa, showing locations of bands discussed in this study.

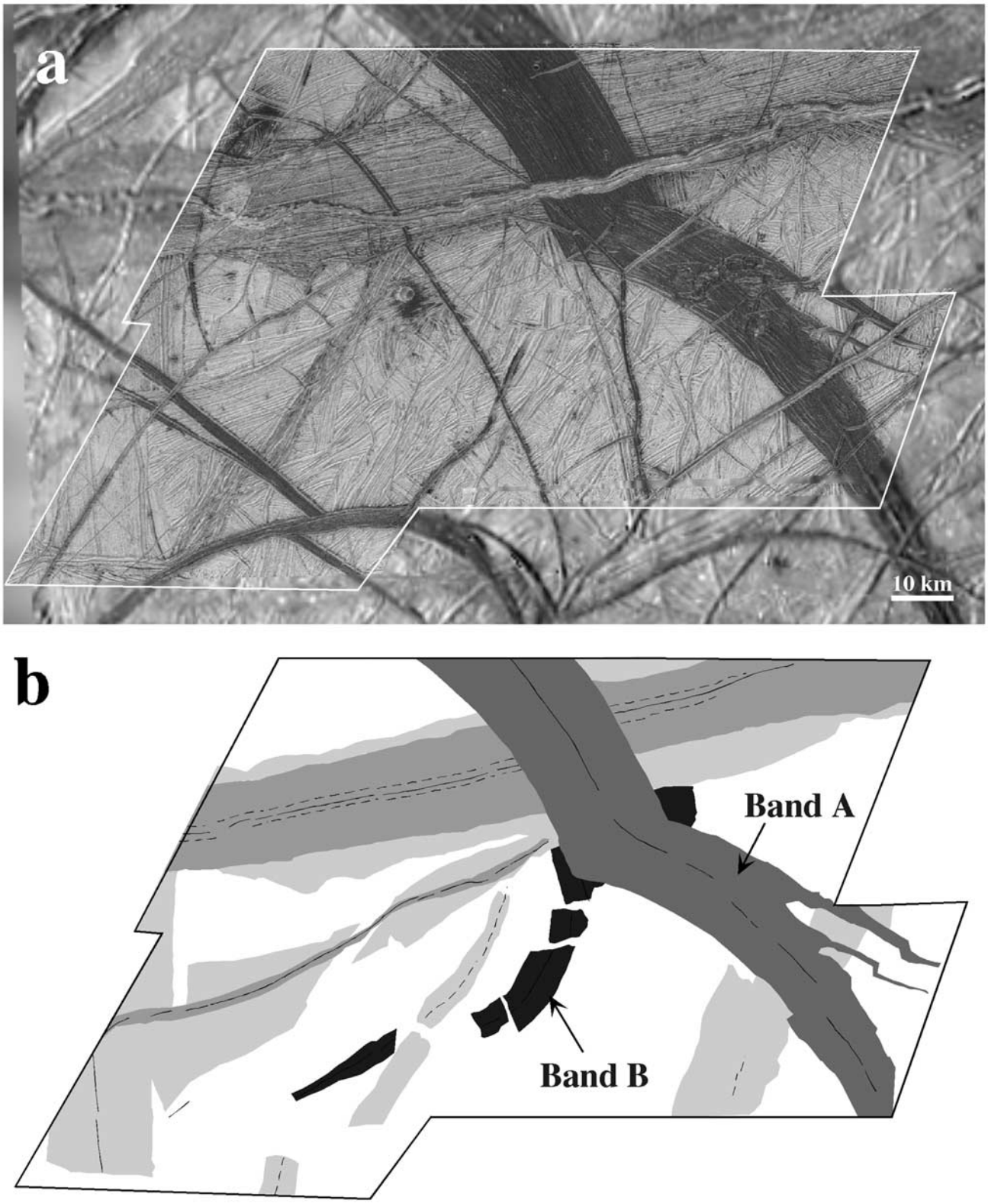


**Figure 2.** Part of the "wedges" area [*Schenk and McKinnon*, 1989] near the Europan anti-Jovian point. (a) This image shows how band albedo correlates with stratigraphic position. The oldest bands are as bright as the background plains and are distinguishable only on the basis of their morphology. Intermediate-aged bands are gray, or intermediate in albedo, such as the wide east-west trending band near the top of the image. The youngest bands have a very low albedo, such as the dark wedge-shaped band trending NW-SE across the image. This high-resolution image (55 m/pixel) from Galileo's twelfth orbit is in a Mercator projection. North is up. (b) Map of all band segments present in high-resolution images, showing that many are offset and crosscut by later bands. Fifty-seven percent of the area outlined in white in Figure 2a has been resurfaced through band formation.

**Table 1.** Galileo Image Data for Bands Investigated in This Study

| | s Clock | Observation | Latitude, deg | Longitude, deg | Incidence, deg | Emission, deg | Phase, deg | Slant range, km | Resolution, m/pixel |
|---|---|---|---|---|---|---|---|---|---|
| Band A | s0426272825 | 12ESWEDGE_02 | −16.2 | 195.7 | 30.0 | 46.7 | 65.7 | 1260.2 | 25.6 |
| | s0426272828 | 12ESWEDGE_02 | −15.8 | 195.4 | 30.1 | 46.1 | 65.7 | 1263.9 | 25.6 |
| | s0426272653 | 12ESWEDGE_01 | −16.7 | 195.8 | 30.1 | 38.0 | 48.0 | 718.8 | 14.6 |
| | s0426272656 | 12ESWEDGE_01 | −16.7 | 195.6 | 30.3 | 37.8 | 48.2 | 725.9 | 14.8 |
| | s0426272661 | 12ESWEDGE_01 | −16.7 | 195.5 | 30.4 | 37.8 | 48.7 | 736.9 | 15 |
| Band A and B | s0426273800 | 12ESWEDGE_03 | −15.8 | 195.0 | 31.0 | 57.2 | 81.4 | 4791.4 | 48.7 |
| stereo context | s0426273813 | 12ESWEDGE_03 | −15.9 | 197.6 | 28.9 | 60.1 | 81.9 | 4900.7 | 49.8 |
| Band B | s0426272642 | 12ESWEDGE_01 | −16.7 | 196.5 | 29.6 | 38.2 | 47.1 | 691.2 | 14 |
| Band C | s0420626752 | 11ESMORPHY01 | 35.4 | 87.8 | 79.7 | 27.9 | 62.4 | 3248.0 | 33 |
| Band D | s0420619265 | 11ESREGMAP01 | −5.97 | 240.1 | 80.4 | 24.1 | 58.2 | 21653.7 | 220 |
| Band E | s0466670513 | 17ESTHYLIN01 | −65.4 | 158.6 | 67.7 | 34.5 | 36.4 | 3784.7 | 38.5 |
| | s0466670526 | 17ESTHYLIN01 | −65.7 | 161.2 | 68.1 | 35.8 | 36.6 | 3798.6 | 38.6 |
| | s0466670539 | 17ESTHYLIN01 | −66.6 | 160.7 | 69.0 | 37.0 | 36.5 | 3811.3 | 38.7 |
| | s0466670552 | 17ESTHYLIN01 | −67.0 | 163.6 | 69.6 | 38.4 | 36.8 | 3829.1 | 38.9 |

of plate-spreading processes that might operate in planetary lithospheres and asthenospheres, and we can tell which aspects of the process can be generalized and which might be specific to Earth. The existence of Europan plate spreading does not imply plate tectonics, however, since subduction zones, an integral part of the terrestrial plate tectonic system, have not been inferred on Europa [*Sullivan et al.*, 1998]. This implies that the overall driving mechanism that formed the Europan bands is likely different from that of primarily "slab-pull"—driven seafloor spreading on Earth [*Forsyth and Uyeda*, 1975].

[4] Regional and high-resolution imaging by Galileo reveals that much of Europa's ridged plains is composed of stratigraphically low bands and ridges that have been crosscut and offset by later features (Figure 2). It has been suggested that features brighten with age [*Pappalardo and Sullivan*, 1996; *Geissler et al.*, 1998], possibly as a result of frost deposition [*Squyres et al.*, 1983] or chemical alteration [*Geissler et al.*, 1998]. Analyses of Galileo images of the anti-Jovian hemisphere indicate that the stratigraphically oldest bands have the same high albedo as the ridged plains and are distinguishable only on the basis of their morphology, while

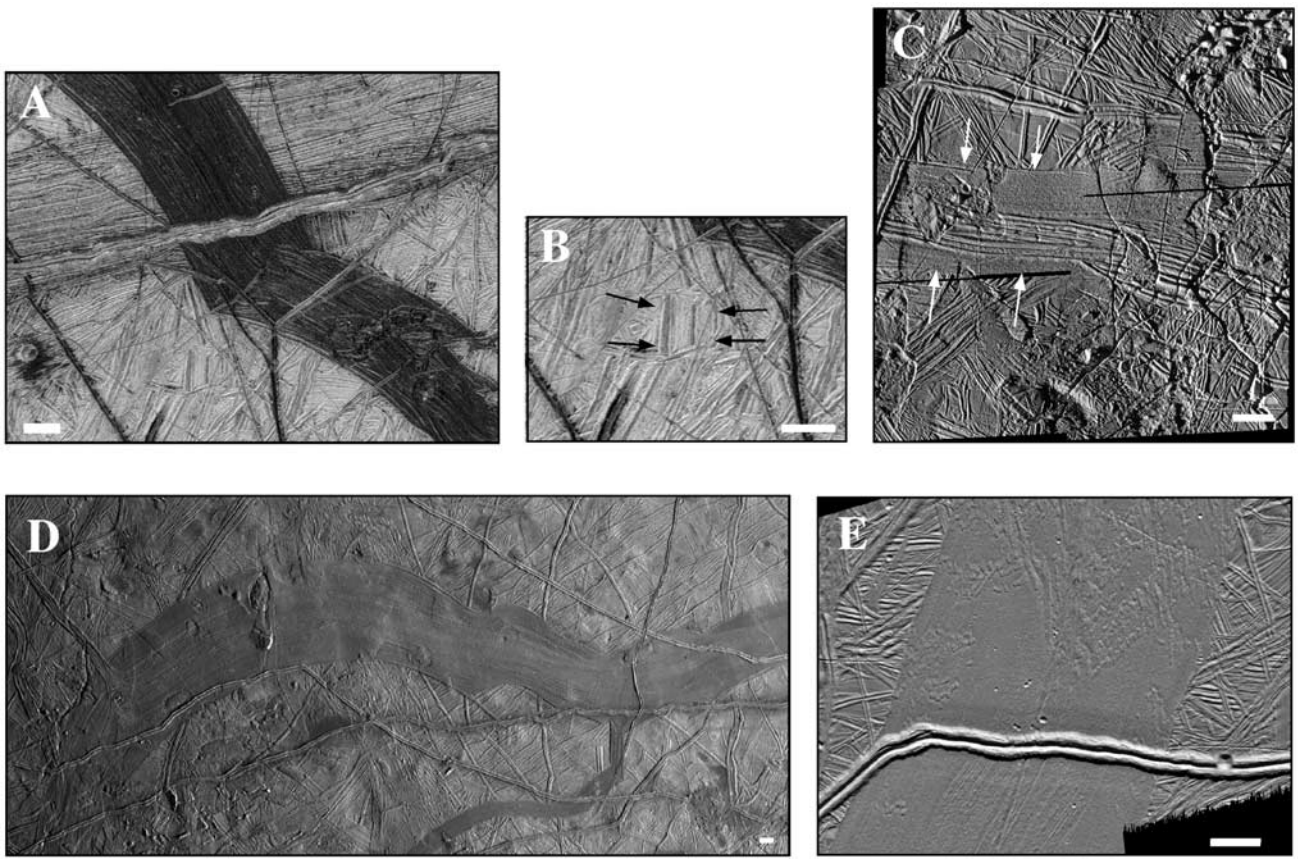


**Figure 3.** Images of the five bands investigated in this study: A, high-resolution low-albedo band; B, high-resolution older, bright band (arrows mark band boundaries); C, high-resolution gray band (arrows mark band boundaries); D, regional-resolution sickle-shaped gray band; E, gray band Thynia Linea. All scale bars are 5 km; north is up.

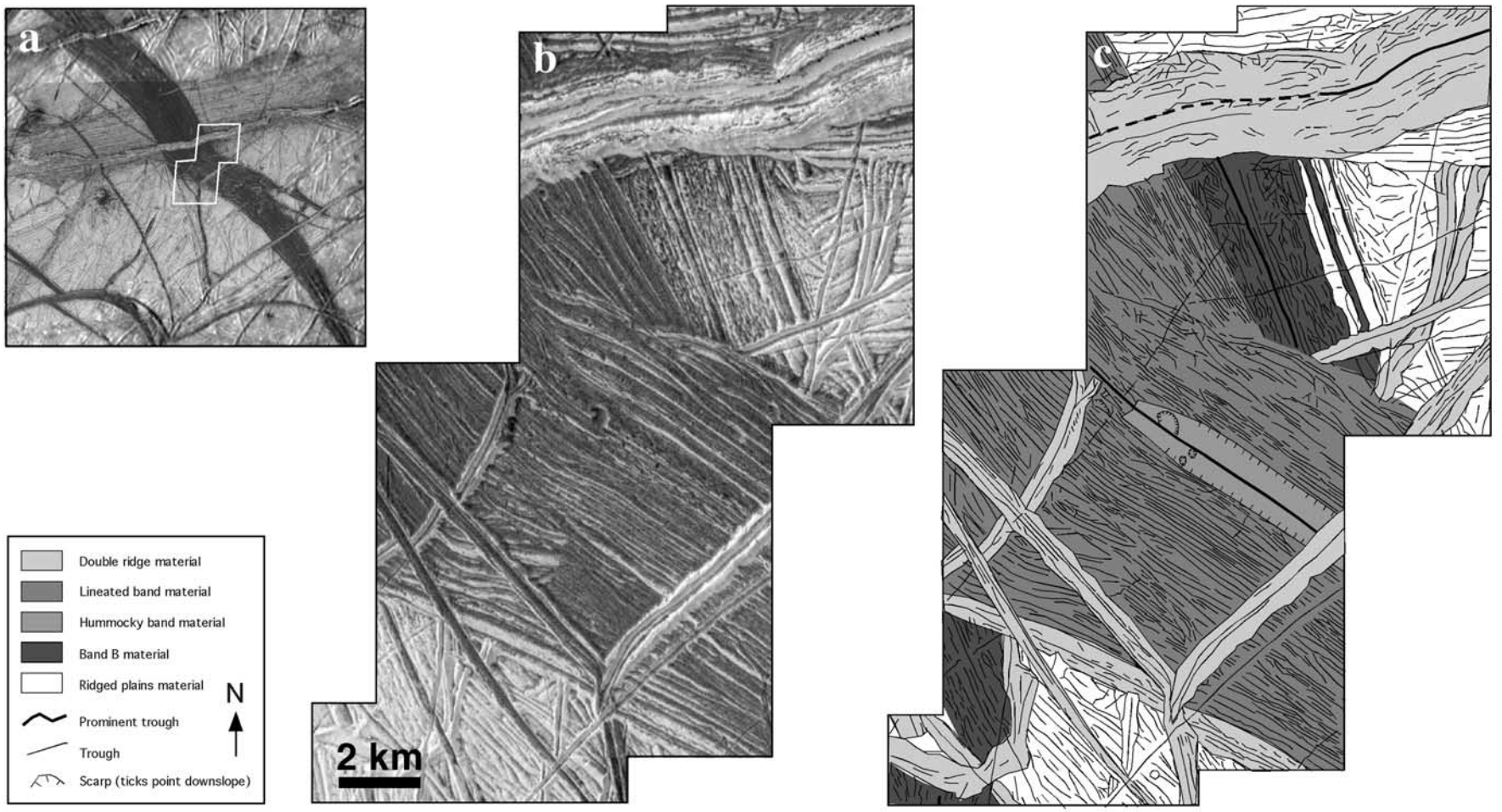


**Figure 4.** Band A. (a) Context image of band A. The white box shows the location of Figure 4b. (b) High-resolution image mosaic (25 m/pixel) of dark band at the point where it changes orientation slightly. The scarp-bounded depression containing the central hummocky zone is observed in stereo imaging and cannot be discerned in this image. (c) Geological sketch map of imaged area.

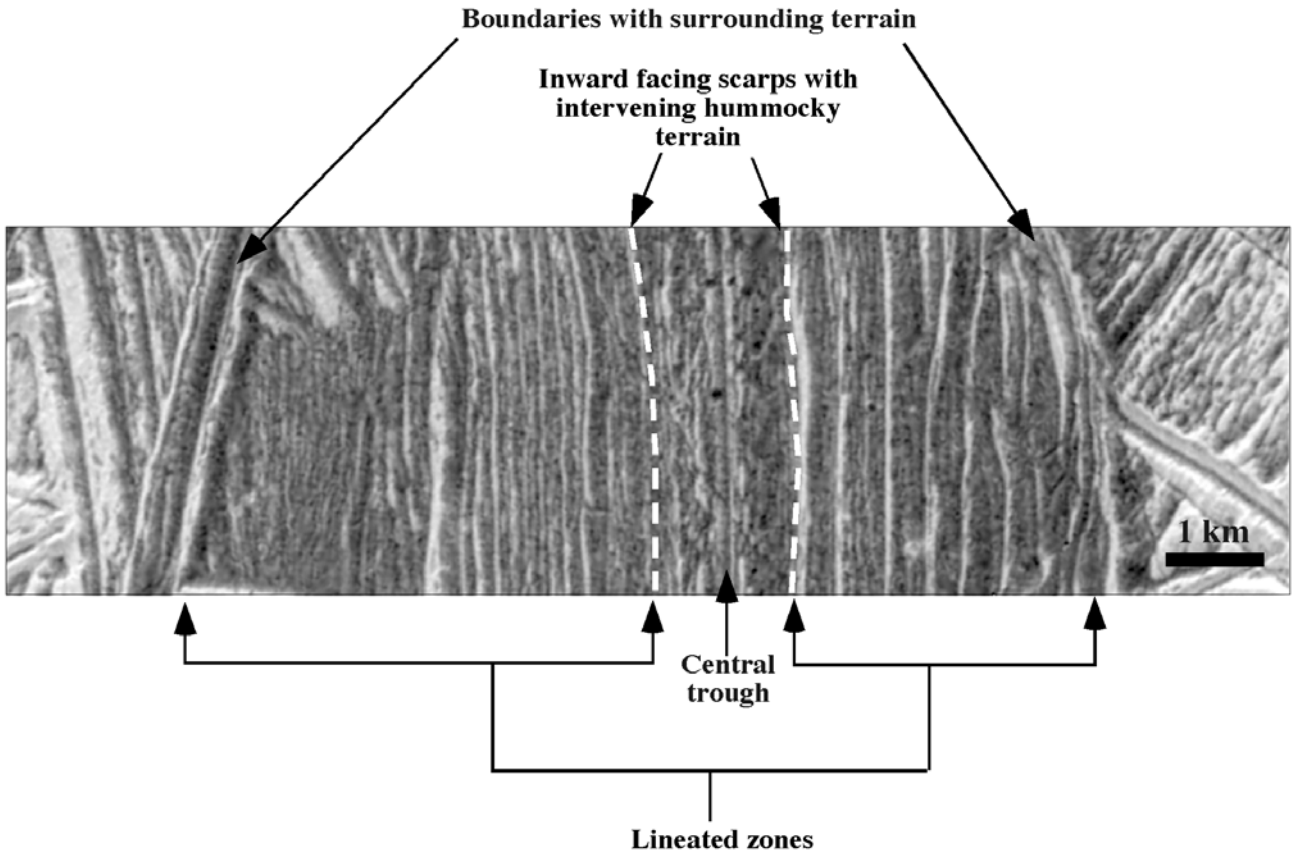


**Figure 5.** Major geological units within band A are broadly similar in width and style on each side of the spreading axis, although small-scale details such as fracture spacing may vary.

intermediate-aged bands are gray and the youngest bands are relatively dark (Figure 2). Brightening with age is consistent with the observed stratigraphy inferred over most of the anti-Jovian region [*Prockter et al.*, 1999]. Mapping of a region southwest of the anti-Jovian point imaged at 55 m/pixel reveals that recognizable bands have resurfaced at least 57% of the area (Figure 2b). The presence of many previously unrecognized bands within the ridged plains confirms the suggestion of *Pappalardo and Sullivan* [1996] that lithospheric separation has been an important means of forming the Europan lithosphere, at least in the anti-Jovian region.

[5] Recent imaging during the Galileo Europa Mission (GEM) allowed several bands to be targeted at resolutions of up to 14 m/pixel, revealing their small-scale interior structure for the first time. Here we analyze the detailed morphologies of Europan bands and conclude that the individual components and their interrelationships have striking similarities to features observed on terrestrial mid-ocean ridges. Detailed mapping reveals distinct morphological units containing linear features and structures, many of which are common among Europan bands. These include an axial V-shaped trough, zones with a rough, hummocky texture, and linear ridges and troughs that we interpret to be tilted fault blocks. The bands show some degree of bilateral symmetry on either side of the axial trough and appear to have spread broadly symmetrically [*Sullivan et al.*, 1998]. The bands may form along preexisting weaknesses in the form of double ridges. Several of the morphological units found along Europan bands are analogous to volcanic and tectonic features observed at Earth's mid-ocean ridges, both in their morphologies and in their volcano-tectonic setting. We find some remarkable similarities, despite compositional differences between terrestrial mid-ocean ridge basalt and Europan ice, and we conclude that the Europan bands form in a manner very similar to terrestrial oceanic rift zones. (In this study we focus on Europan "pull-apart" bands as defined in the Voyager sense [e.g. *Schenk and McKinnon*, 1989], rather than triple bands or complex ridges, which have very different morphologies and likely different formational mechanisms [e.g. *Schenk and McKinnon*, 1989; *Fagents et al.*, 2000; *Figueredo and Greeley*, 2000].)

[6] *Tufts et al.* [2000] propose that bands form as a consequence of opening and closing of ice fractures in contact with a liquid water ocean less than a few kilometers below the surface. In their model, liquid water freezes within fractures penetrating to the liquid ocean just below, and varying amounts of secular and diurnal tidal activity result in the formation of different band morphologies. However, several problems have been noted concerning the viability of surface-ocean interactions across such a thin brittle shell as explanations for surface morphologies [e.g., *Crawford and Stevenson*, 1988; *Pappalardo et al.*, 1999; *Collins et al.*, 2000; *Gaidos and Nimmo*, 2000; *Prockter and Pappalardo*, 2000; *Stevenson*, 2000]. In this paper we explore the concept that bands on Europa form primarily through solid-state deformation that occurs within a thicker icy shell than the model proposed by *Tufts et al.* [2000].

## 2. Morphology of Bands on Europa

[7] The Galileo spacecraft has imaged several different bands on Europa at varying resolutions and lighting geometries. We mapped details of five bands imaged at 14–220 m/pixel (Table 1, Figures 1 and 3). These examples are representative of different band morphologies at different resolutions. Band A is dark and stratigraphically young and was imaged in stereo with sufficient resolution to reveal small-scale structure. Band B is one of the stratigraphically

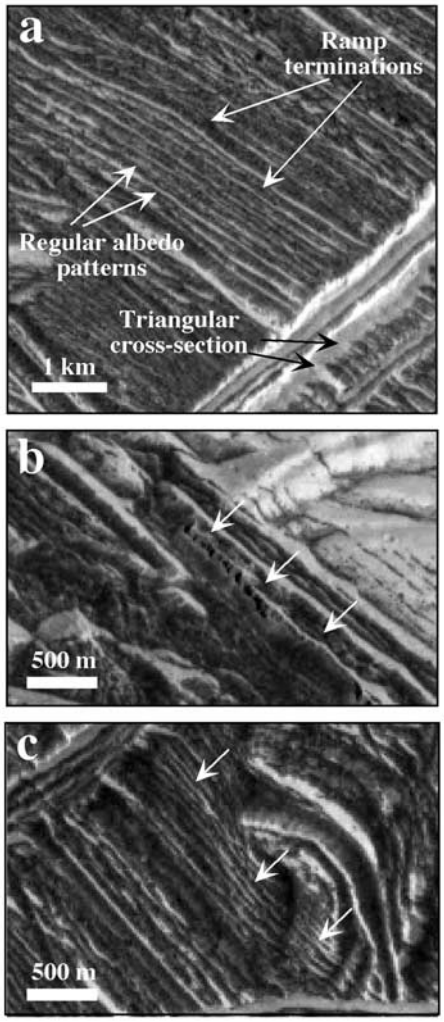


**Figure 6.** Detail of band A, from high-resolution Galileo imaging. (a) Linear features showing regular albedo striping, apparent triangular cross sections where crossed by a later forming ridge, and ramp terminations, all of which imply a tectonic origin. North is up. (b) Small scarp (arrows) with talus deposits at foot. North is down. (c) Fine-scale fissures close to center of band. North is up.

oldest bands studied and is as bright as the surrounding ridged plains. The band's high relative albedo and the availability of excellent image resolution allow its interior features to be easily distinguished. In addition, stereo imaging was obtained across one portion of the band. Band C is an intermediate-albedo gray band, imaged at sufficient resolution for comparison to bands A and B. B and C appear to have only one dominant morphological unit and have been disrupted by later tectonic events. Band D is a wide, sickle-shaped gray band, imaged at 220 m/pixel. This band was studied to determine how much morphological detail documented at high-resolution could also be distinguished at lower resolution. Band E is a prominent band, Thynia Linea, first mapped and reconstructed from Voyager images by *Pappalardo and Sullivan* [1996]. At high resolution, Thynia exhibits an unusual chevron-like pattern of small hills on its surface, unlike any of the other bands imaged [*Sullivan et al.*, 1999a].

[8] We first describe the internal morphologies and bounding structures observed within and along these five bands and discuss their similarities and differences. Next we compare the morphological features of Europan bands with those observed along terrestrial mid-ocean ridges and offer an interpretation for the mode of their formation.

### 2.1. Band A: Dark Band at High Resolution

[9] Galileo imaged a wedge-shaped band centered at ~17°S, 197°W (Figures 1, 3a, and 4) at 420 m/pixel and higher resolutions up to 15 m/pixel (Table 1). *Sullivan et al.* [1998] and *Tufts et al.* [1997] showed that the low-albedo material comprising this band could be removed and the margins could be reconstructed almost perfectly. Figure 4b shows high-resolution images obtained by Galileo, centered on a "dogleg," a region where the band abruptly changes orientation from SSE to ESE. Band A measures ~18 km across at this dogleg. Along the central axis of the band is a narrow but well-defined axial trough [*Sullivan et al.*, 1998; *Tufts et al.*, 2000], ~100 m wide (Figures 4b and 4c). The trough appears to be V-shaped in profile, is extremely linear, and approximately bisects the imaged portions of the band.

[10] Bilateral symmetry of lineaments within band A was first noted by *Sullivan et al.* [1998], who noted that the trough corresponds to the axis of symmetry. Higher-resolution imaging reveals broad symmetry of other units on either side of the axial trough (Figure 5). Distributed out to an equal distance (~1 km) on either side of the axial trough are many small hill-like features, or hummocks. These are elliptical in plan view, with long axes parallel to the axial trough and measuring a few hundred meters.

[11] The main body of the band outside the central hummocky zone is characterized by linear features oriented along the trend of the band (Figures 4 and 5). *Sullivan et al.* [1998] suggested that bilateral symmetry of these features was due to ridges and troughs that formed originally at the center of the band in material with

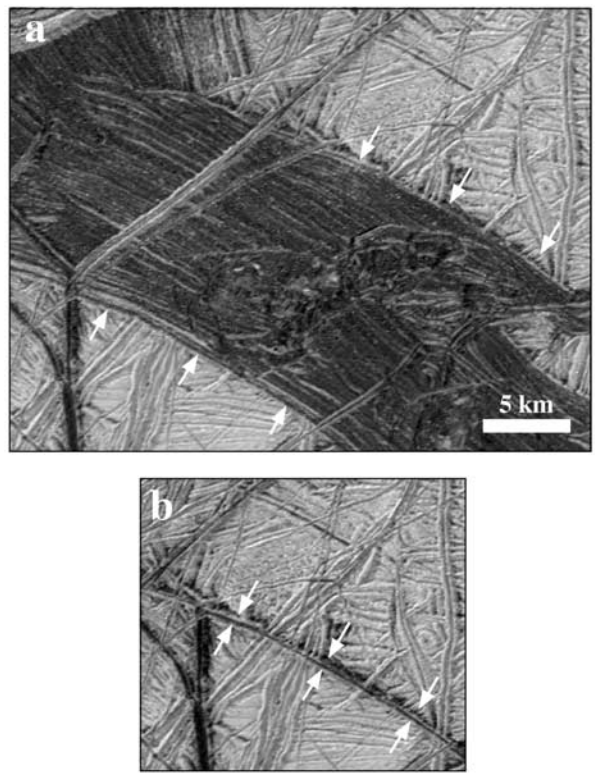


**Figure 7.** (a) Image of the portion of band A just below the point where it doglegs. (b) When the intervening band material is removed and the margins are reconstructed, it becomes apparent that band A initiated along a double ridge similar to those ubiquitous on Europa's surface. Arrows are in the same position along the band margin in both images.

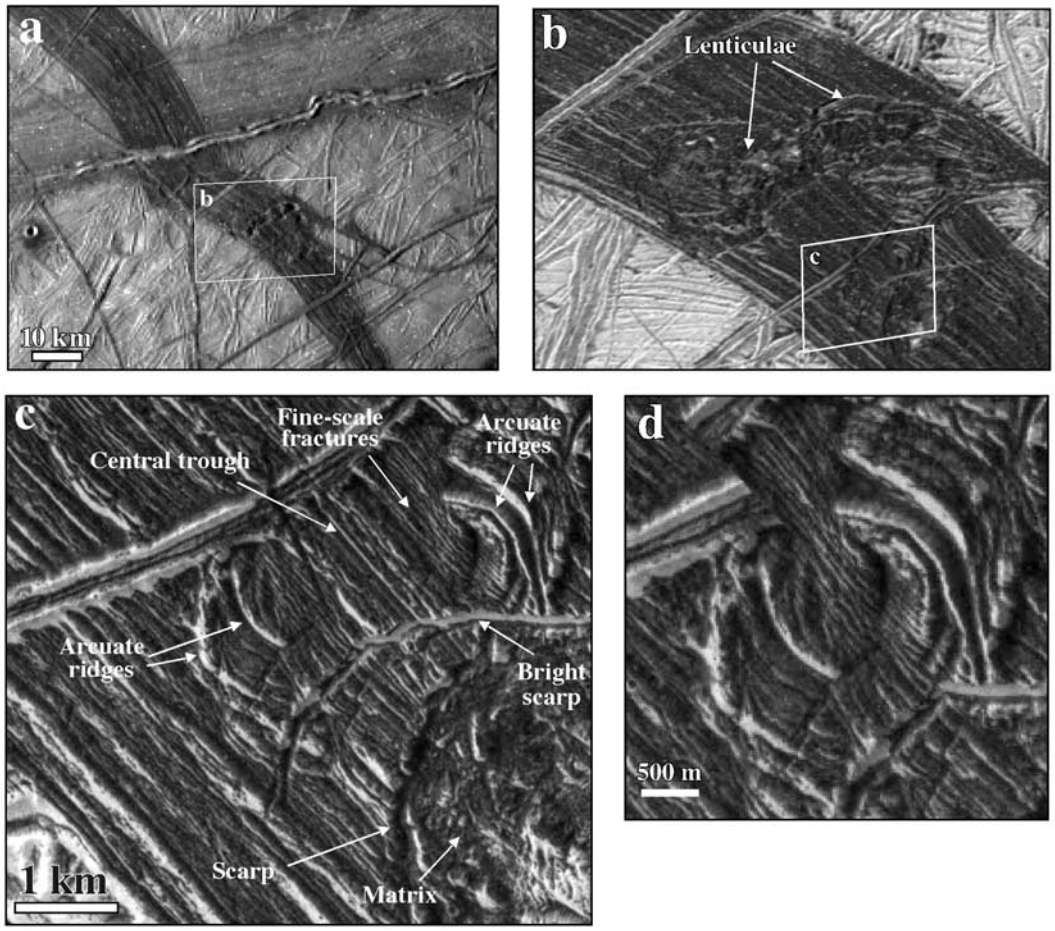


**Figure 8.** (a) Regional image of band A. The box shows the location of Figure 8b. (b) Regional Galileo image showing series of collapse features across the band, interpreted to be lenticulae with microchaos texture. The white box shows the location of Figure 8c. (c) High-resolution image of lenticula and associated scarps within band A. Note subcircular ridges that have been separated across the spreading axis. (d) Reconstruction showing possible preoffset configuration of subcircular ridges.

sufficient viscosity (or which stiffened rapidly after emplacement) to retain these structural signatures during migration away from the band axes. Higher-resolution Galileo images reveal that detailed morphology within units, such as the spacing of finer-scale lineaments, may vary on either side of the band.

[12] Much of the band material appears to have been tectonically disrupted. Linear features are found to have even spacing and repetitive high- and low-albedo patterns (Figure 6a). Where crosscut by later features such as double ridges, triangular cross sections are revealed and ramp terminations are common. These observations all imply a tectonic origin for these small-scale lineaments, indicating that the material of the band has been broken up into tilted fault blocks. At one place along the band there is a well-defined scarp, which appears to have a talus pile at its base (Figure 6b). Similar styles of mass wasting have been observed elsewhere on Europa [*Sullivan et al.*, 1999b; *Head et al.*, 1999a]. Very high resolution imaging (15 m/pixel) reveals closely spaced parallel lineaments that we interpret to be fissures, as they appear to "slice up" the background terrain (Figure 6c).

[13] The boundary between the main body of band A and the surrounding plains is defined on the southwestern side by a prominent double ridge (Figure 4). Below the dogleg the northern edge of the band appears to be bounded by a single ridge, less prominent than the southern bounding ridge. Figure 7 shows a reconstruction in which the low-albedo band material just south of the dogleg has been removed and the preexisting features on each side of the band have been reconstructed. The reconstruction indicates that at least for this part of the band, a double ridge appears to have been exploited during band formation, such that each ridge crest has become a bounding ridge on either side of the band. On the basis of this reconstruction, the region south of the dogleg where the band changes its orientation has been offset in a right lateral sense by ~5 km. The outline of band A implies that it formed by exploiting one of Europa's cuspate ridges, which are scalloped in plan view [*Hoppa et al.*, 1999a].

[14] Several subcircular features are present within band A; these were identified as "pit complexes" by *Sullivan et al.* [1998] from regional-resolution imaging on Galileo's third orbit (Figure 8a). Closer examination of the high-resolution images (Figure 8b) shows that these features are examples of postemplacement deformation by lenticulae [*Carr et al.*, 1998; *Pappalardo et al.*, 1998a; *Greeley et al.*, 1998]. Lenticulae are subcircular domes, depressions, or areas where the preexisting terrain has been disrupted into small blocks and matrix material, collectively known as "microchaos" [*Head et al.*, 1997, 1998; *Pappalardo et al.*, 1998a; *Spaun et al.*, 1998]. Figure 8c shows the interior of one of these features at 15 m/pixel, revealing a sharp subcircular scarp bounding a rough, hummocky-textured matrix. This feature appears to have disrupted the preexisting material of the band into microchaos, as several linear features are sharply truncated by its bounding scarps. One possible mechanism for lenticulae

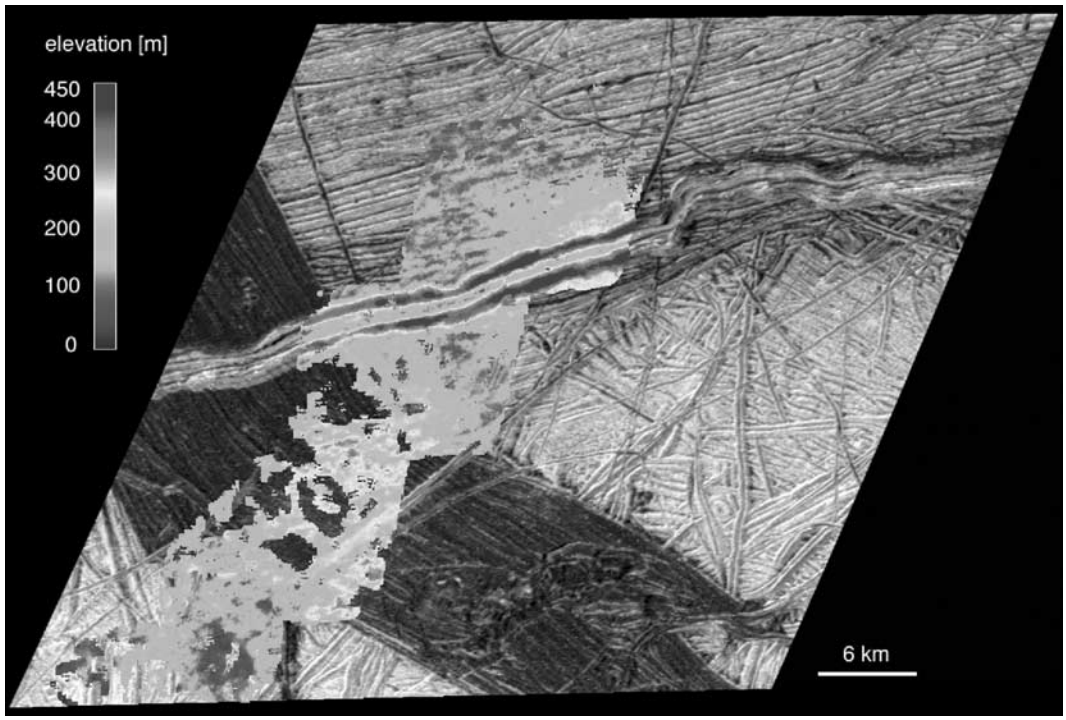


**Figure 9.** Digital terrain model of band A showing height differences of up to 100 m between the band and the surrounding plains. See color version of this figure at back of this issue.

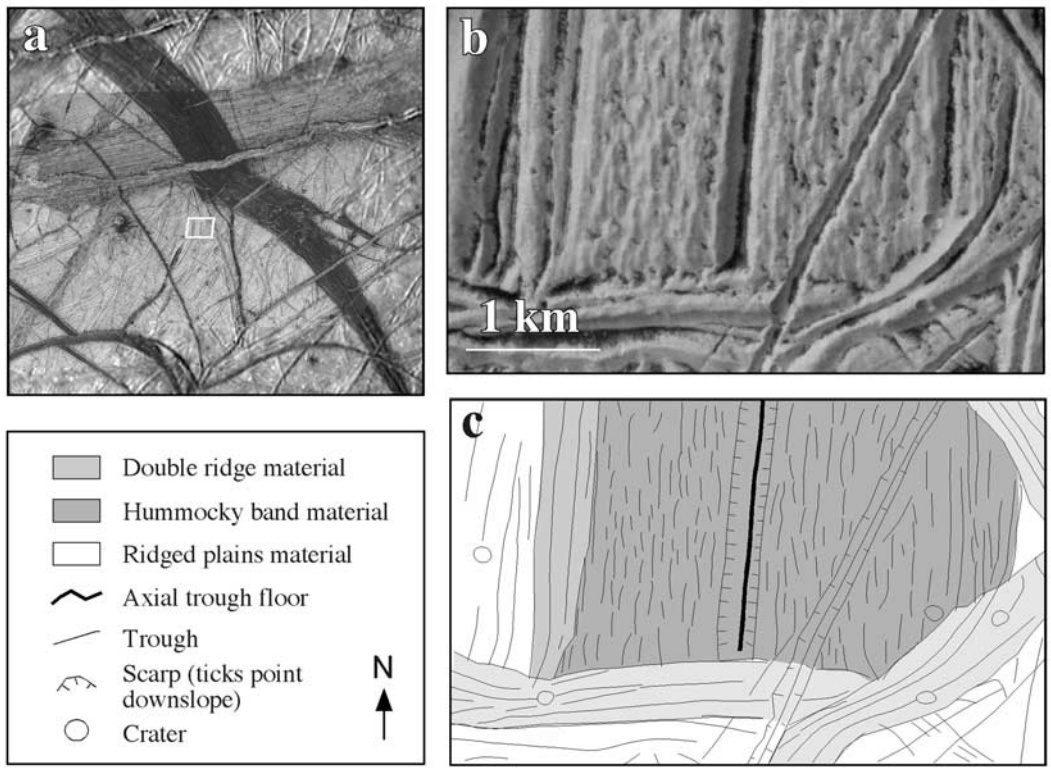


**Figure 10.** Band B. (a) Location of high-resolution image. The white box shows the location of Figure 10b. (b) High-resolution image (14 m/pixel) of relatively old, bright band showing hummocky unit and distinct axial trough. (c) Geological sketch map of imaged area.

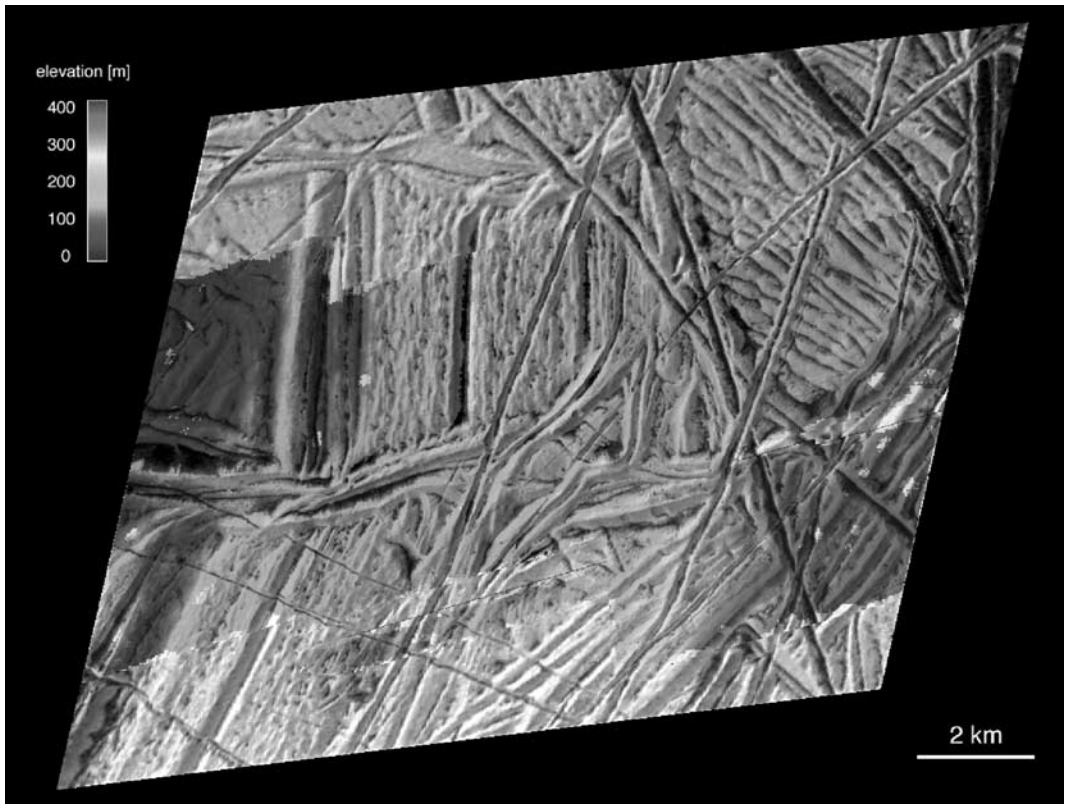


**Figure 11.** Digital terrain model of band B showing no distinct height variations across the band but a regional slope rising from west to east. See color version of this figure at back of this issue.

formation is the interaction of warm ice diapirs with the colder, brittle surface [*Pappalardo et al.*, 1998a]. Lenticulae are observed to postdate the majority of Europan stratigraphic units imaged in some areas of Europa [e.g., *Prockter et al.*, 1999; *Figueredo and Greeley*, 2000], and they may represent a change in the thermal state of Europa's ice shell over recent geological time [*Pappalardo et al.*, 1998b]. If band A is relatively young, as expected given its relatively low albedo [*Pappalardo and Sullivan*, 1996;

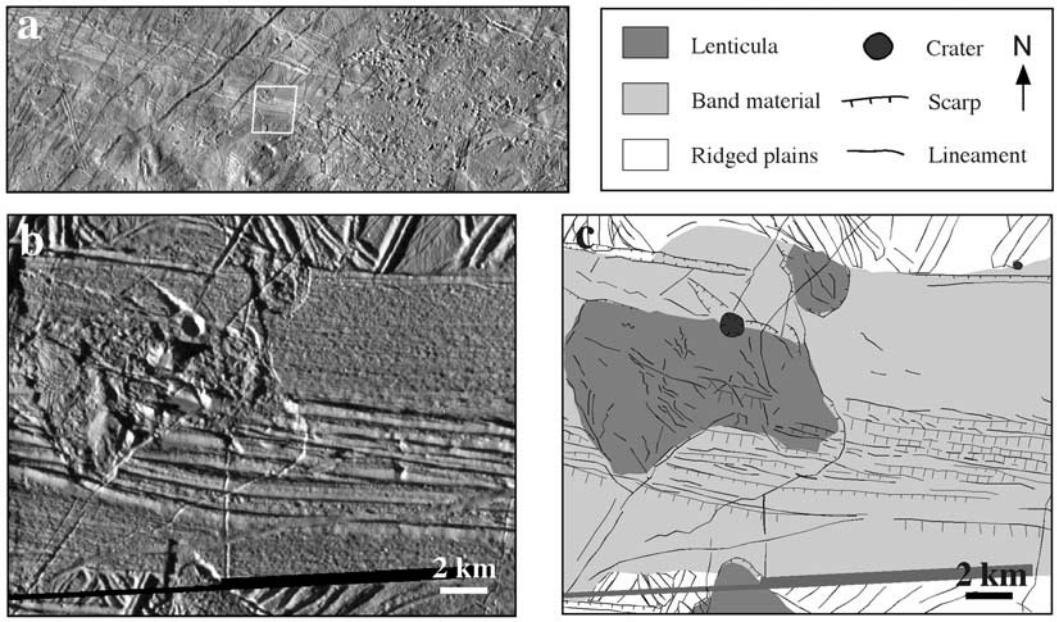


**Figure 12.** Band C. (a) Context image of band C. The white box shows the location of Figure 12b. (b) High-resolution image of band C (33 m/pixel). The texture at this resolution is hummocky at small scales, with some visible lineations. The band itself appears relatively flat, other than the tilted fault blocks. The band is disrupted to the left of the image by a lenticula. (c) Geological sketch map of band C.

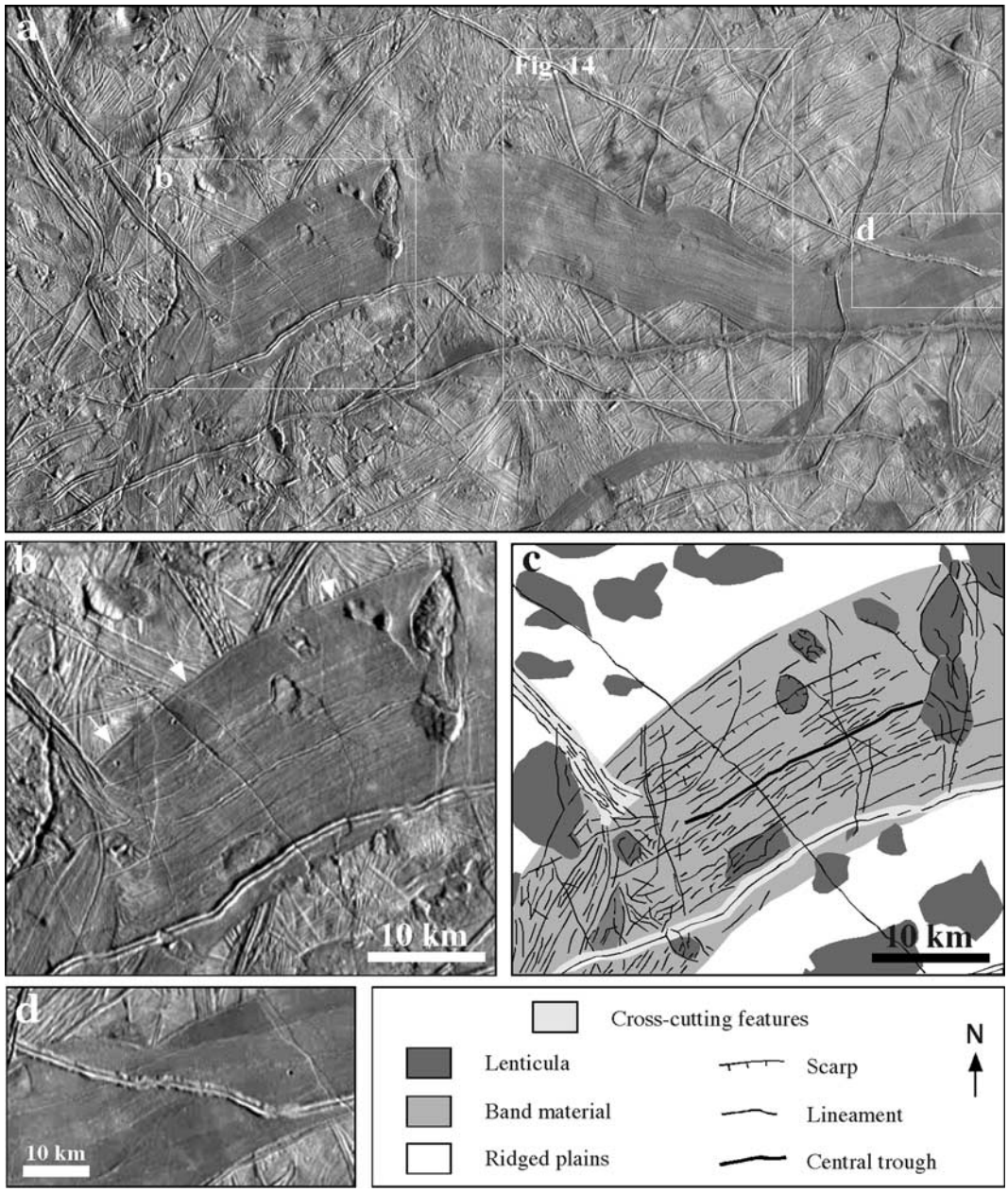


**Figure 13.** Band D. (a) Context image of band D. The white boxes show the locations of Figures 13b, 13d, and 14. (b) Portion of gray band showing lineaments, albedo variations, and lenticulae as discussed in the text. Arrows point to the bounding ridge. (c) Geological sketch map of Figure 13b. (d) This image illustrates the change in the morphological characteristics of a younger double ridge as it crosses band D. The ridge is crisp and well defined when traversing the ridged plains (see Figure 14a) but becomes ill defined when crosscutting the band material.

*Squyres et al.*, 1983; *Geissler et al.*, 1998], then the lenticulae are probably among the youngest geological features in the region [*Head et al.*, 1999b]. Although the lenticulae have clearly disrupted preexisting band material, their distribution in a line perpendicular to the band trend is consistent with initial formation during the spreading process. We suggest that the lenticulae underwent subsequent modification as, or after, they moved away from the central axis.

[15] In addition to the lenticulae, there are some sets of arcuate ridges located beyond equal distances of ~1 km on either side of the axial trough in band A; the ridges are concave toward the axial center of symmetry (Figure 8c). When intervening band material is removed and right-lateral offset is reconstructed, the arcuate ridges match up to form a subcircular shape (Figure 8d). These ridges do not appear to be impact-related; neither do they exhibit the characteristic morphology of lenticulae (scarps surrounding a depression filled with hummocky-textured material). The ridges may possibly be the surface expression of a lenticula that impinged on the band during the spreading process but did not interact sufficiently with the surface to disrupt it into microchaos. The right-lateral offset across the entire band is ~5 km, but these arcuate ridges are offset by only ~1 km. Given their distance from the axial trough (~1 km), this suggests that the dextral offset observed along the whole band is distributed across the width of the band, rather than occurring along a single fault; that is, the band opened obliquely. It is unclear if spreading occurred with new material moving in a constant, oblique direction away from the axis or if spreading occurred in small increments normal to the axis, interleaved with small episodes of

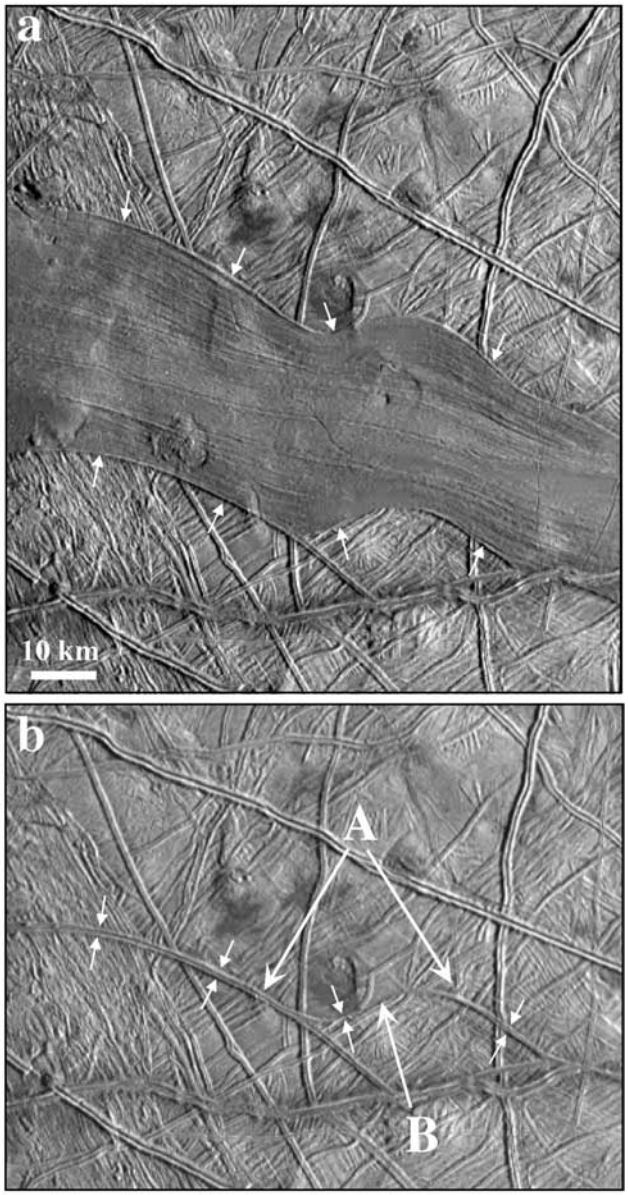


**Figure 14.** Reconstruction of band D. (a) Band D prior to reconstruction of margins. (b) Reconstruction showing that band D appears to have formed by exploiting at least two preexisting double ridges (A). Band formation appears to have linked an area between the ridges (B). Arrows are in the same position along the band margin in both images.

strike-slip motion, perhaps along the structural grain of troughs and ridges evident throughout the band area. Whatever the precise mechanism, the net effect has been that material has moved obliquely away from its origin along the spreading axis.

[16] A digital terrain model (DTM) has been constructed from stereo images obtained during Galileo's twelfth orbit (Figure 9), according to the method outlined by *Giese et al.* [1998]. The DTM resolves features $\geq$400 m with vertical resolution of $\sim$20 m. The model covers a transect across the center of the band and shows that the band stands higher than the surrounding plains by 50–100 m (Figure 9). The smallest ridges superimposed on the band are up to 100 m higher still. The stereo images reveal that the axial trough and hummock fields are contained within a flat, topographically low area extending $\sim$1 km to either side of the trough that is bounded by inward facing scarps. This region is only slightly depressed, probably by no more than a few tens of meters, and is unresolved in the DTM shown in Figure 9.

### 2.2. Band B: Older, Bright Band at High Resolution

[17] A narrow bright band was imaged by Galileo at regional and high resolutions on its twelfth orbit (Table 1; Figure 10); band B measures $\sim$6 km at its widest and is crosscut and offset by band A. Portions of band B can be seen immediately to the northeast and south of band A in Figure 4. Here we concentrate on one small section of the band imaged at 14 m/pixel. Band B shows some of the same morphological units as band A, and the morphology is easier to distinguish because of the band's higher relative albedo, which is the same as the surrounding ridged plains. Band B is offset into several segments by subsequent ridge and band formation (Figure 2b), and this overprinting by later tectonic activity prevents determination of the extent of any shear across the band during its formation.

[18] The axial trough in band B is well developed and extremely linear; the V-shaped morphology is more apparent in the high-resolution imaging (Figure 10b). The trough is $\sim$400 m wide but narrows to <100 m across the floor. A zone of hummocks extends almost all the way from the axial trough to the margins. The elliptical hummocks are commonly $\sim$100 m wide perpendicular to the central axis and 200–800 m in the along-axis direction. No flat areas are visible between the hummocks; they are immediately adjacent to each other. Some low-albedo material is visible in topographic lows between them. Later crosscutting troughs have obscured the eastern band margin, while on the western margin a prominent ridge is visible, bounding the band (Figure 10b). The axial trough and bounding ridge can still be discerned in lower-resolution images of this band, and these features appear to persist elsewhere along the band (e.g., Figure 2).

[19] A digital terrain model (DTM) of band B (Figure 11) with 10 m vertical resolution indicates that there is a regional slope across the band, such that the eastern half stands over 100 m higher than the western margin. The western boundary is at an elevation similar to the adjacent ridged plains. Implications of the topography of this band are discussed in section 5.5.

### 2.3. Band C: Gray Band at High Resolution

[20] Band C is located in Europa's leading hemisphere and was imaged at high resolution (33 m/pixel) during Galileo's eleventh orbit (Figure 12; Table 1). Reconstruction across this $\sim$14 km wide gray band shows that it has been offset by $\sim$10 km in a right-lateral sense [*Tufts et al.*, 2000]. The band consists of rough-textured, somewhat lineated material composed of small, subcircular hummocks <200 m in diameter. Some faint striations are present within the textured material, oriented parallel to the band margins. Band C has well-defined boundaries, in some places delineated by a small scarp on the northern side (Figure 12b), and preexisting ridges are abruptly truncated at both margins of the band.

[21] There are several clearly defined ridges within the band that are about 1 km wide. These ridges appear to have a triangular cross section, with one bright (sunlit) face exhibiting scarp-like morphology, while the backtilted face has the same albedo and hummocky texture as undisrupted portions of the band (Figure 12b). The inferred scarps are consistently south facing. On the basis of this morphology, these lineaments are interpreted to be south verging tilt blocks [*Prockter et al.*, 1998; *Figueredo and Greeley*, 2000] formed by normal faulting due to continued extension during the formation of band C. These blocks are morphologically similar to the scarp identified in band A (Figure 6b).

[22] Subsequent modification of band C has occurred through the formation of a lenticula with a "microchaos" interior texture. No axial V-shaped trough is observed in band C, although much of the central axis of the band has been disrupted by the tilted fault

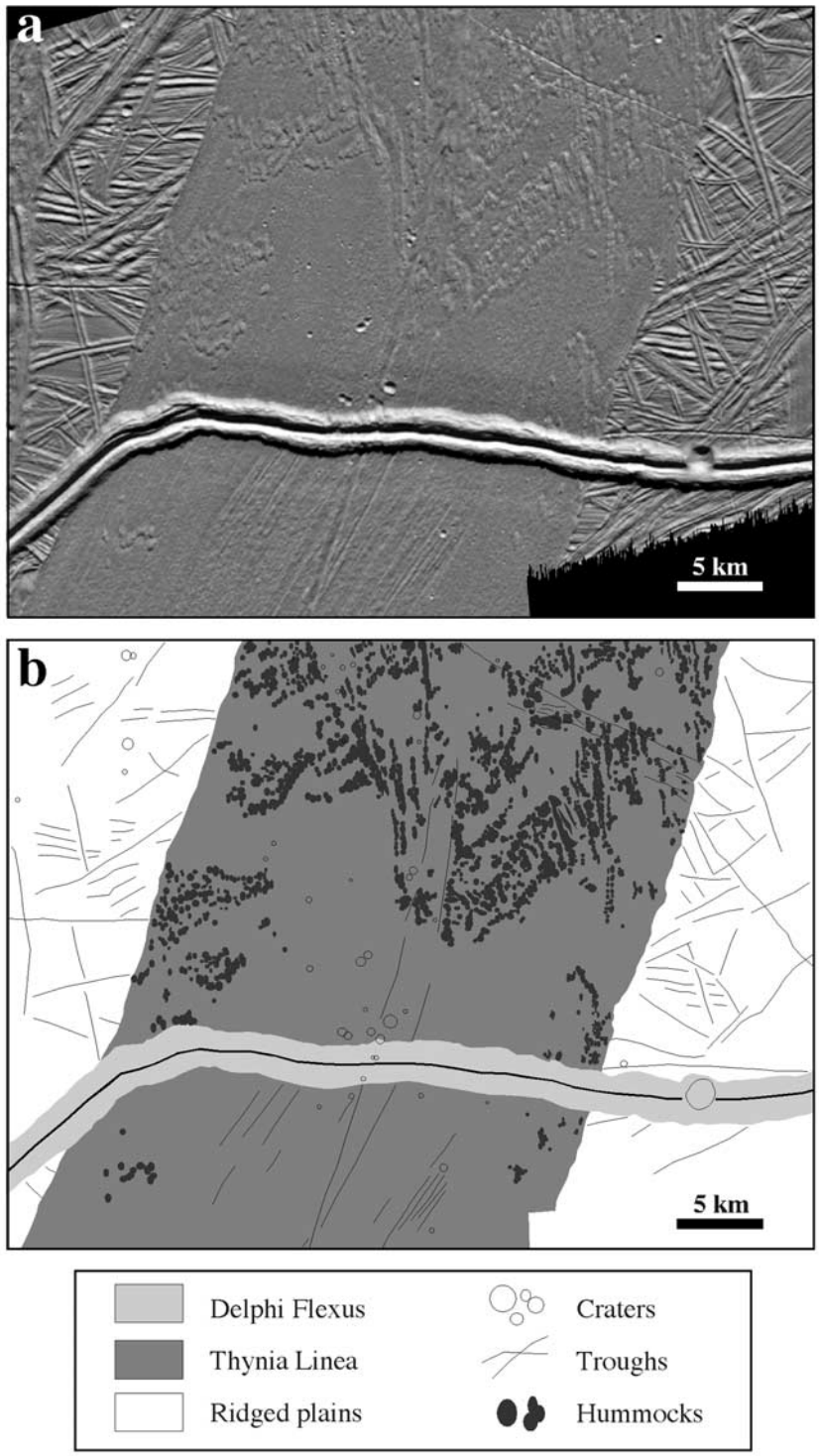


**Figure 15.** (a) Galileo image of Thynia Linea showing small hummocks arranged in chevron patterns. The large double ridge crossing from east to west is Delphi Flexus. North is up. (b) Geological sketch map of Thynia Linea.

blocks and the formation of the lenticula, and so any trough present may have been disrupted beyond recognition.

### 2.4. Band D: Sickle-Shaped Gray Band at Regional Resolution

[23] A sickle-shaped gray band imaged during Galileo's eleventh orbit at 220 m/pixel (Figure 13) has a maximum width of ~20 km. In band D an axial trough is clearly visible despite much lower resolution imaging than for bands A and B (Table 1). This trough is located near the central axis of the band and is subparallel to, but more linear than, its curvilinear margins. Several lineaments are present and are more or less distinctive along different parts of the band (Figures 13b and 13c).

[24] Band D can be divided into three swaths on the basis of relative albedo and structural associations. The central swath is

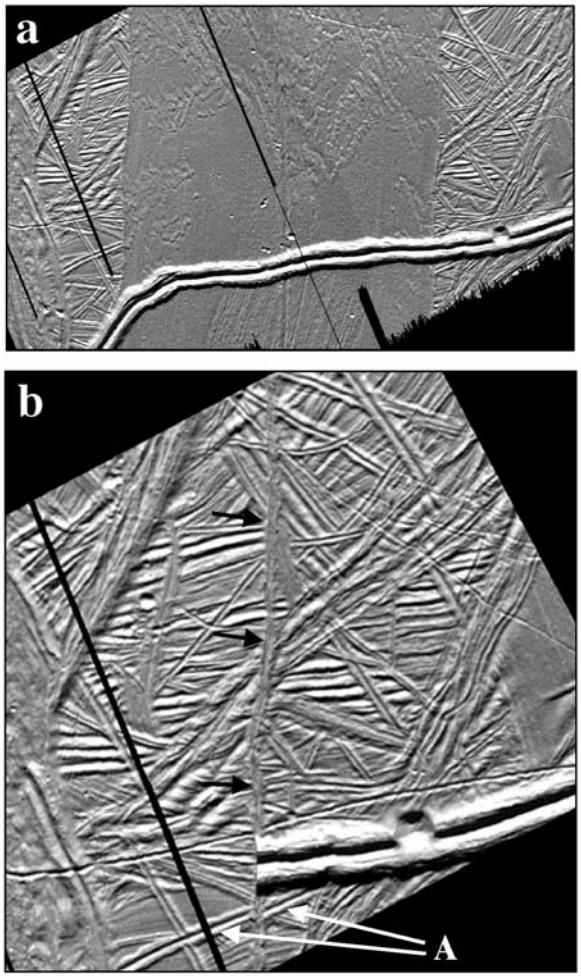


**Figure 16.** (a) Thynia Linea, before removal of band material and reconstruction of margins. (b) Reconstruction of Thynia margins showing that the band appears to have formed along an ''immature'' double ridge or fracture, with indistinct margins (black arrows). Note that the ridge shown by A can be reconstructed with virtually no offset, despite the fact that it is north of Delphi Flexus on the western margin of Thynia, and south of Delphi on the eastern margin of Thynia, prior to reconstruction. This implies that the formation of Delphi Flexus has not extended or compressed the terrain upon which is has formed, an observation that places constraints on models of ridge formation.

~10 km across, with a slightly higher albedo and lineaments that are straighter than are the band margins, while the flanking outer swaths are each ~5 km wide, somewhat darker, with curvilinear outer margins. The band has been partially disrupted by cross-cutting fractures, double ridges, and lenticulae. No axial relief or hummocky material can be resolved within the band at this scale, although the central swath appears to have a rougher texture than the outer swaths.

[25] Parts of the band are ridge-bounded (e.g., arrows, Figures 13b and 14a). When the band material is removed, allowing the margins to be reconstructed, it is clear that these individual bounding ridges are segments of two separate preexisting double ridges along which the band appears to have initiated (A of Figure 14b). Areas where there are no ridges along the band margins may be places where a fracture linked the ridge segments exploited during band formation (B of Figure 14b). The band appears to have opened in a north-south direction, perpendicular to the trend of its margins, in which case there has been virtually no strike-slip offset along the east-west trending portion of the band.

### 2.5. Band E: Large Gray Band Thynia Linea

[26] Thynia Linea is 25 km wide and extends for over 900 km, making it one of the largest gray bands recognized in Voyager images. *Pappalardo and Sullivan* [1996] identified Thynia Linea as a region of lithospheric separation and infilling by darker material, and Galileo imaged part of the band at ~38 m/pixel on its seventeenth orbit (Table 1). In addition to the hummocky zones common within bands, a different class of hummocks is present within the gray band material of Thynia Linea (Figure 15). Thynia has a uniform intermediate albedo, small-scale hummocky texture, and linear structures (Figure 15a). South of Delphi Flexus these lineaments are parallel to each other but are subparallel to the band margins, implying that the opening direction may not always have been uniform along the band. The spreading axis is not marked by the prominent V-shaped trough observed in several other Europan bands. Thynia Linea is not bounded by ridge crests but appears to have initiated within preexisting ridged plains. Figure 16 shows a reconstruction of the margins of Thynia once the intervening band material has been removed. The bounding ridge crests that remain once the band has been closed (Figure 16) are small, ill defined, and diffuse, suggesting that Thynia formed along a relatively undeveloped or immature ridge or a fracture. Reconstruction shows that there has been ~500 m of right-lateral offset along the band.

[27] Thynia Linea has on its surface several distinct chains of hummocks (Figure 15). These individual hummocks are typically >500 m long and are arranged in chevron patterns that are largely bilaterally symmetric [*Sullivan et al.*, 1999b]. *Sullivan et al.* [1999b] propose that these hummocks formed at the spreading axis of Thynia and then were split asymmetrically as the band spread apart. These workers further suggest that small asymmetries in the distribution of hummocks across the band imply a reorientation of the spreading axis by different amounts from 7° to 10°.

## 3. Comparison of Europan Band Morphologies

[28] We have examined five Europan bands: a young dark band, an older bright band, a gray band (all imaged at high resolution), a sickle-shaped gray band imaged at regional resolution, and a large distinct gray band, Thynia Linea, which displays some unusual morphological characteristics. There are distinct similarities in the morphological units observed among all the bands imaged by Galileo, suggesting that the bands may have a common mode of formation.

### 3.1. Axial Trough

[29] High-resolution imaging of different bands shows that the center of symmetry corresponds roughly to the axial trough, present in bands A, B, and D, and we interpret this as the place at which new band material has been created with spreading proceeding to each side.

### 3.2. Hummocky Texture

[30] All bands imaged at high resolution exhibit hummocky textures, although the exact nature of these textures varies among bands. Within band A (Figure 4), the hummocky zone is confined to an area lying within a topographically low valley, ~1 km wide on either side of the axial trough. On bands B and C (Figures 10 and 12) the hummocky region extends across the entire width of the band, may be lineated in places, and generally has a uniform albedo. Thynia Linea (band E; Figure 15) exhibits two scales of hummocks: (1) a small-scale background hummocky texture and (2) larger, well-developed elongated hummocks arranged in bilat-

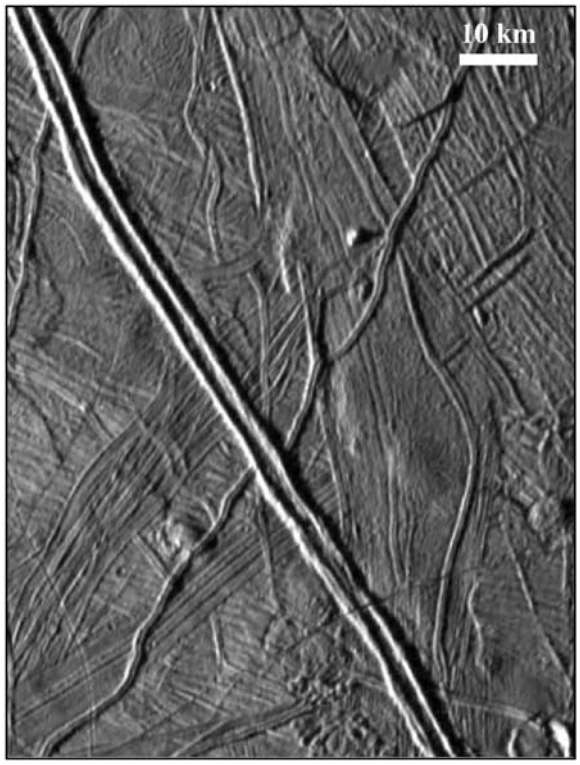


**Figure 17.** Galileo image of double ridge near the impact feature Tyre Macula. Note the separation between the ridge crests, showing new material on the floor in between.

erally symmetric chevron patterns on either side of the axial trough.

### 3.3. Subparallel Linear Structures

[31] Regardless of resolution, each of the bands has linear structures that are parallel or subparallel to the band margins. Many of these linear features are interpreted to represent ridges and troughs that formed in relatively viscous material at the band axis and then migrated away from the band axis [*Sullivan et al.*, 1998]. Individual ridge and trough morphology may vary as a response to minor variations in spreading rate. In some cases these features appear to have undergone subsequent tectonic disruption into fault blocks and fissures. In band A, structures are interpreted to be fractures and tilted fault blocks on the basis of their regular albedo patterns, scarp faces, triangular cross sections, and ramp terminations (Figures 6a–6c). Band C (Figure 12) shows evidence of tilt block formation. In band D (Figure 13), linear textures parallel or subparallel to the band margins may indicate subresolution tectonic structures. Where observed, faulted terrain does not necessarily appear on both sides of the spreading axis, and faults may have different spacing at different places along or across a band.

## 4. Relationship of Bands to Ridged Plains

### 4.1. Boundaries With Surrounding Plains

[32] Each of the bands has distinct boundaries with their surroundings. In bands A, B, and D (Figures 4, 10, and 13) each margin is marked by a single ridge rising above the surrounding plains. These single bounding ridges resemble one half of a typical Europan double ridge of the same approximate dimensions [*Greeley et al.*, 1998]. The presence of bounding ridges similar to half of a double ridge suggests that double ridges provide sites of preexisting weakness where band formation begins. A double ridge near the Tyre impact structure has partly separated crests, resulting in a flat medial floor between (Figure 17). This ridge appears to be "frozen" in a state of incipient band formation. *Prockter et al.* [2000] observed ridges bounding parts of Agenor Linea and proposed that this band formed when dextral strike-slip movement was initiated along a preexisting weakness, most likely a cycloidal double ridge.

[33] Other bands may initiate along fractures rather than double ridges. In bands C and E (Figures 12 and 15) the boundary with the surrounding plains is relatively sharp and occurs at the edge of the hummocky band material. Removal of the central material comprising band E (Thynia Lynia) and refitting of its margins reveal that it opened along a line of weakness in the form of a low ridge that appears to be hardly more than a raised-flank fracture, with very indistinct margins (Figure 17).

### 4.2. Features Formed Subsequent to Band Formation

[34] All of the bands imaged by Galileo have crosscutting tectonic features, especially double ridges (e.g., Delphi Flexus in Figure 15) and narrow troughs that probably represent fractures (e.g., within band B, Figure 10). In some cases a crosscutting ridge has less well defined crests and margins while crossing the band than on the ridged plains (Figure 13d). We speculate that this indicates that the ridge formed not long after the band, when the band material was still relatively warm and less capable of supporting significant topography.

[35] Other features that have formed subsequent to band formation are lenticulae [*Carr et al.*, 1998; *Pappalardo et al.*, 1998a; *Greeley et al.*, 1998], which may take the form of depressions, domes, or regions of microchaos (e.g., bands A and D, Figures 8 and 13). The development of microchaos after band formation is well illustrated in band C (Figure 12), where microchaos has disrupted the preexisting texture of the band such that it is unrecognizable. In band A a line of lenticulae has formed parallel both to the inferred direction of spreading and to two crosscutting ridges. We do not find any examples of lenticulae that are split and separated by any of the bands studied, suggesting that band formation preceded lenticulae formation in all of the areas studied.

### 4.3. Topography

[36] A digital terrain model of band A (Figure 9) shows that the band material is elevated with respect to the surrounding plains. *Tufts et al.* [2000] report stereo analysis indicating that dark bands other than those used in this analysis also stand higher than the surrounding plains. Moreover, Thynia Linea was noted in Voyager images as standing slightly above its surroundings [*Pappalardo and Sullivan*, 1996]. The fact that some bands stand higher than their surroundings suggests compositional or thermal buoyancy, a point to which we will return in section 5.5.

### 4.4. Relative Albedo

[37] Band A (Figure 4) is significantly darker than other bands studied here, although some of the linear structures within the band appear to have bright crests. Elsewhere on Europa, dark material is observed to shed downslope and may reveal brighter material below, triggering thermal segregation of the surface and resulting in extreme albedo heterogeneity [*Spencer et al.*, 1998; *Pappalardo et al.*, 1998c; *Sullivan et al.*, 1999b; *Head et al.*, 1999a]. Alternatively, the bright crests may be the result of frost deposition [*Squyres et al.*, 1983]. Band B (Figure 10) is essentially indistinguishable from the bright ridged plains and is one of the oldest bands mapped; its high relative albedo and low position in the local stratigraphic column compared with band A are consistent with the prediction that bands brighten with age. Bands C and E (Figures 12 and 15) both have a remarkably uniform albedo, although variations may not be recognizable because of the high incidence angle at which these images were obtained (Table 1). Band D (Figure 13) was imaged at a similar incidence angle to bands C and E (Table 1) and also has an intermediate albedo, although the central swath of

**Table 2.** Comparison Between Europan Bands and Terrestrial Mid-ocean Ridges

| Europan Bands | Terrestrial Mid-ocean Ridges |
|---|---|
| *Similarities* | |
| upwelling and emplacement of new lithospheric material | upwelling and emplacement of new lithospheric material |
| broadly symmetrical spreading | broadly symmetrical spreading |
| central axial trough | central axial trough (fast-spreading ridges) |
| tilted fault blocks | abyssal hills |
| hummocks | axial volcanic ridges, Seamounts |
| shear offset along bands | oblique spreading at some ridges |
| topographically high | situated at crest of topographic rise |
| *Differences* | |
| driving force probably related to tidal cycle; does not appear to be related to subduction | driven primarily by slab-pull force resulting from subduction |
| no apparent segmentation | segmentation/topographic variations along length of ridge (less pronounced at fast-spreading ridges) |

the band is somewhat brighter. The relative albedos of the bands are consistent with their position in the local stratigraphy, although it is difficult to determine their relative stratigraphy on a regional or global scale given the small areas imaged by Galileo and uncertainties in our knowledge of frost deposition.

### 4.5. Oblique Opening of Bands

[38] Shear displacement has been observed along several of the bands studied. Reconstruction of band A (Figure 4) shows that 5 km of right-lateral offset has occurred, and this shear appears to be distributed across the width of the band. The offset across Band A may be accounted for in part by the fact that the imaged area is on a cusp where the band changes orientation. Spreading perpendicular to the band direction north of this cusp would result in dextral offset to the south. It is not possible to tell from the segments of band B (Figure 10) still visible within the ridged plains whether it has undergone any offset along its length, because it has been so heavily overprinted and displaced by subsequent ridged plains formation. Band C (Figure 12) has undergone right-lateral displacement of ~10 km during opening [*Tufts et al.*, 2000]; band D (Figure 13) does not appear to have any significant component of opening; and band E (Thynia Linea, Figure 15) has a dextral shear component equivalent to ~500 m of offset along the imaged area. In some Europan bands, such as Astypalaea Linea, oblique opening is clearly indicated by the band's lensoid outline [*Tufts et al.*, 1999]. In others, such as the bands studied here, oblique opening may be the net result of small episodes of spreading normal to the axis, interleaved with increments of strike-slip motion. Since many of the bands imaged show evidence of lineaments and tilted fault blocks, it is likely that some of the shear component of band opening may have been accommodated by these structures. Variations in the amount of offset among the bands do not appear to be correlated with differences in the morphological features or structures present within them (such as the size of hummocks).

## 5. Comparison Between Europan Band Morphologies and Terrestrial Mid-ocean Ridges

[39] Each morphological unit discussed in section 3 is common to at least three of the five bands studied, suggesting that they are fundamental units resulting from the band formation process. On the basis of these observations, we now address the similarities and differences between Europan bands and Earth's mid-ocean ridges (i.e., oceanic rift zones), the site of terrestrial seafloor spreading.

[40] On Earth the majority of new lithosphere is created at mid-ocean ridges by buoyant upwelling and generation of partial melt of the upper mantle. This material is emplaced at and near the surface by magma-filled cracks and solidifies to form oceanic crust and lithosphere. The global average thickness for terrestrial oceanic crust is 5–6 km [*Chen*, 1992]. Similar volcanic and tectonic units are observed at different mid-ocean ridges, but detailed morphology varies with spreading rate and magma supply [*Morgan and Chen*, 1993]. The similarity between the style of rifting on Europa and terrestrial mid-ocean rift zones was first suggested by *Schenk and McKinnon* [1989] and was reinforced by *Sullivan et al.* [1998], who noted the bilateral symmetry of internal features within band A. Very high resolution Galileo images further reveal the striking similarity between units identified within Europan bands and morphologies found at terrestrial mid-ocean ridges (Table 2).

### 5.1. Axial Trough

[41] The morphologies created during terrestrial seafloor spreading vary widely according to spreading rate and magma supply [*Malinverno*, 1990; *Morgan and Chen*, 1993; *Small*, 1998; *MacDonald*, 1998]. A deep axial rift valley is almost always present at slow spreading ridges, such as the Mid-Atlantic Ridge (0–5 cm/yr, full rate) (Figure 18a). This axial valley is composed of a series of nested graben with walls as close as 1 km to the axial rift, with the entire rift valley measuring 20–40 km across the shallowest point between the bounding scarps [*MacDonald*, 1982]. The average depth of this axial valley is ~1.4 km. At fast spreading rates such as along the East Pacific Rise (9–16 cm/yr), an axial high is always present, and no rift valley occurs, only a narrow (<200 m) axial summit trough, or caldera [*Lonsdale*, 1977; *Ballard et al.*, 1988; *MacDonald and Fox*, 1988]; topography is relatively smooth with a fine-scale horst and graben structure (Figure 18b) [*MacDonald*, 1982]. At intermediate spreading rates (5–9 cm/yr) the axis may have either a rift valley or an axial high.

[42] A model proposed by *Sinton and Detrick* [1992] consistent with seismic and petrological data suggests that magma chambers are composed of narrow, hot, crystal-melt mush zones. Pure melt develops only at fast spreading ridges, where enough magma is present to form a thin lens of melt at the top of the mush zone (Figure 18b). At slow spreading ridges, insufficient magma is present to develop a melt lens, so eruptions on these ridges are periodic, occurring only when there are influxes of melt from the mantle. The magma mush zone may extend continuously for tens of kilometers along the ridge crest at fast spreading centers but may be only tens or hundreds of meters thick (Figure 18a). Investigations of mid-ocean ridge seismic structure have revealed a strong correlation between the cross-sectional form of a ridge and the presence or absence of a magma chamber close to the surface (see *Forsyth* [1993] for review). Increased supply of magma leads to shallow magma chambers and a corresponding broadening of axial topography (the "axial high"), as seen at fastspreading ridges.

[43] Several hypotheses have been proposed to account for the presence or absence of the axial rift valley. One of these is the

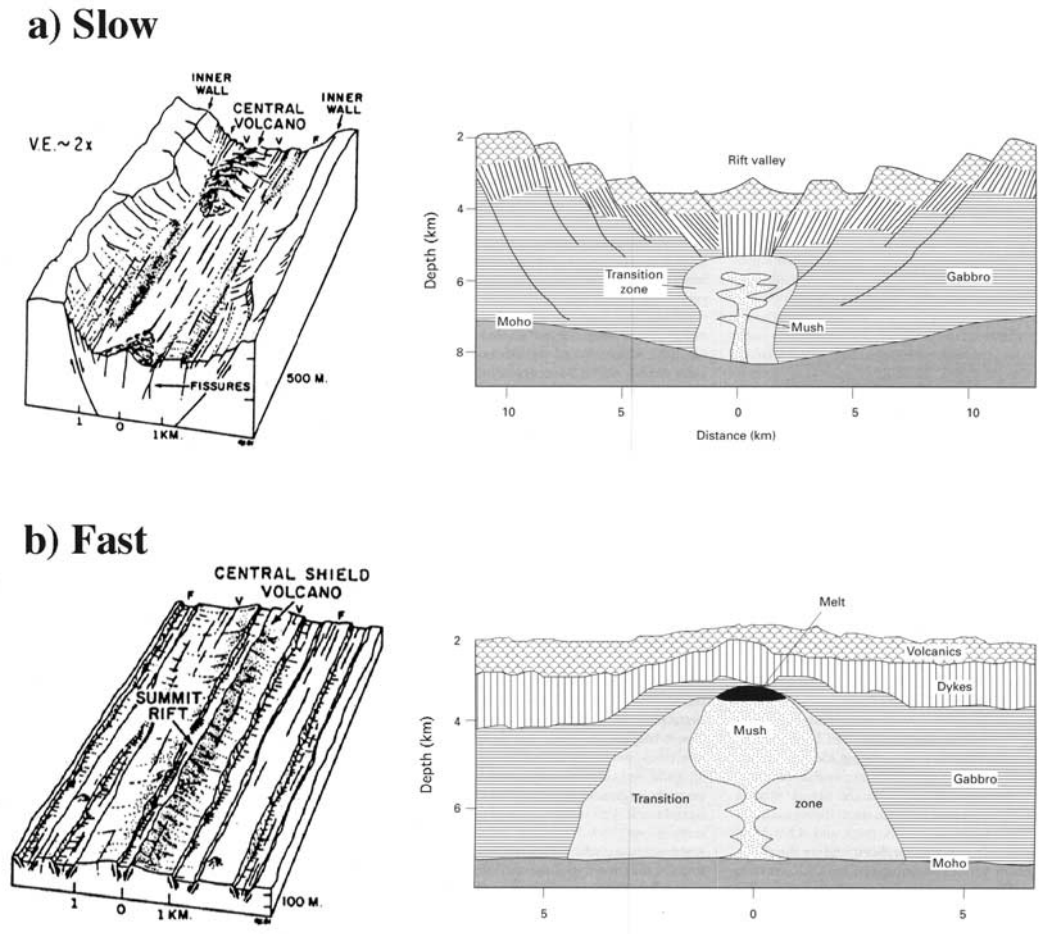


**Figure 18.** (left) Morphological features and (right) interpretive models of corresponding magma chambers found at (a) slow-spreading terrestrial mid-ocean ridges and (b) fast-spreading terrestrial mid-ocean ridges. (Morphological models are from *MacDonald et al*. [1982], with permission, from *Annual Review of Earth and Planetary Sciences*, Volume 10, ©1982 by *Annual Reviews* (www.AnnualReviews.org); magma chamber models from *Sinton and Detrick*, 1992].)

hydraulic head model [*Sleep*, 1969; *Lachenbruch*, 1973; *Sleep and Rosendahl*, 1979], in which viscous forces within a conduit from the magma source are sufficiently large to cause a decrease in hydraulic pressure. This causes a depression directly over the ridge axis while simultaneously causing uplift of the axial valley walls relative to the floor. A second model is one of "steady state" necking of the lithosphere [*Tapponier and Francheteau*, 1978], in which necking in a ductile layer beneath the rift causes the formation of an axial valley. This may result in significant topography beneath slow spreading ridges, while the crust at fast spreading ridges is thought to be too hot and weak for necking to have any significant effects.

[44] The Europan axial troughs are analogous to terrestrial axial summit troughs because in each case the axis is where new material is emplaced onto the surface, although smaller-scale details of their morphology and formation may be different. Several Europan bands have a prominent, linear axial trough running approximately down their centers, and material on either side of this axial trough consists of units of similar texture and width from the trough out to the margins. This strongly suggests that the bands are spreading roughly symmetrically from a central axis, as is generally the case at Earth's mid-ocean ridges.

[45] One interpretation for the origin of the central caldera on the East Pacific Rise is that it has a collapse origin [*Fornari et al.*, 1998] (see section 5.2). Although superficially similar morphologically, it is unlikely that the Europan axial troughs represent collapse features. One reason for this is the difficulty of sustaining a liquid close to the surface of Europa [e.g., *Pappalardo et al.*, 1999]. At Galileo resolutions the Europan troughs do not show any of the morphological features generally associated with collapse, such as a sinuous outline and scalloped margins. Instead, they appear to be remarkably linear with relatively distinct and apparently unmodified margins, implying a tectonic origin. The troughs are likely faults possibly resulting from the spreading process or possibly from shear focused along the zone of weakness at the spreading axis.

### 5.2. Extrusive Features

[46] Within the central axial valley is the region of active volcanism known as the neovolcanic zone, estimated to be 1–3 km wide along the slow spreading Mid-Atlantic Ridge and rarely wider than 3 km at other spreading centers, regardless of spreading rate [*MacDonald*, 1982]. The majority of volcanism occurs within the axial rift valley (at slow spreading rates) or from the trough at the crest of the axial high (at fast spreading rates). Some off-axis volcanism occurs also; this is estimated to be <10% at one area studied along the slow spreading Mid-Atlantic Ridge [*MacDonald*, 1986] and has also been observed along the East Pacific Rise [*Fornari*, 1986; *Perfit and Chadwick*, 1998].

[47] The style of volcanism at fast spreading ridges appears to be dominated by volume-limited sheet flows, leading to low-relief

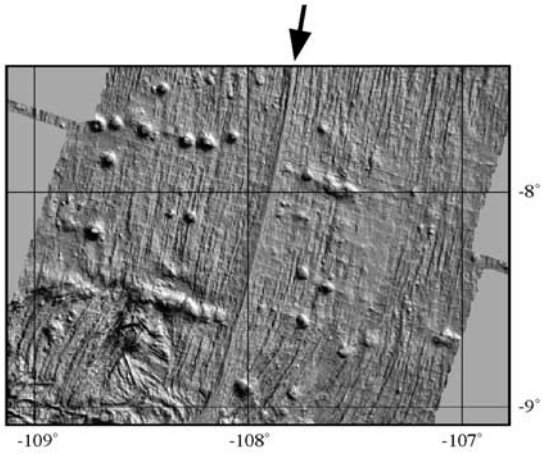


**Figure 19.** Gridded bathymetry image of the East Pacific Rise from ~7.5° to 9°S. Round features are seamounts (after *Cochran et al.* [1993] and the RIDGE Multibeam Synthesis Project (http://coast.ldeo.columbia.edu/general/html/home.html)). Arrows point to the location of the central axial trough, and lineaments are normal-faulted abyssal hills.

topography and ponding [*Bonatti and Harrison*, 1988; *Perfit and Chadwick*, 1998; *Head et al.*, 1996], although seamounts may also be formed [e.g., *Scheirer and MacDonald*, 1995].

[48] On faster spreading ridges the narrow elongate depressions common at the ridge crest (Figures 18b and 19) are sites at which new ocean crust is created by magmatism and subsequently modified by tectonism [e.g., *Haymon*, 1996]. *Fornari et al.* [1998] propose that the trough has a primary volcanic/magmatic origin and forms as a response to the collapse of shallow lava flow surfaces over zones of primary eruptive fissures and subsurface lava tubes and channels. Alternatively, *Chadwick and Embley* [1998] propose that this summit rift is a dike-induced graben structure on the basis of observations associated with recent eruptive events.

[49] The surface expression of volcanism at slow spreading ridges commonly occurs in the form of axial volcanic ridges (AVRs) [*Searle and Laughton*, 1981] and seamounts [*Smith and Cann*, 1992; *Smith et al.*, 1995]. AVRs are large (tens of kilometers long, hundreds of meters high) convex ridges, ellipsoid in plan view, composed of many different volcanic flows (Figures 18a and 20), while seamounts tend to be less elliptical (Figure 19) and may be a constituent of AVRs. AVRs are rooted in faults and fissures within the neovolcanic zone, and the volcanic edifices which pile up to form AVRs likely result from cooling-limited, rather than volume-limited, flows [*Head et al.*, 1996]. Axial volcanic ridges and seamounts may be analogous to the hummocks observed in some Europan bands. The Europan hummocks appear far more numerous and closely spaced than terrestrial volcanic features, however [*Jacoby*, 1980; *Parson et al.*, 1993]. If hummocks formed by a mechanism similar to terrestrial AVRs, their scale difference may result from differences in the extrusion process of ice compared to that of molten rock. With ice, progressive upwelling and chilling of new material would be superimposed onto continued cracking and extension of the band. This new material may have been sufficiently viscous, as a result of composition or cooling, to form small domes built up on the chilling margins of the extruded band material (which may itself be composed of gentle ridge and trough terrain, e.g., section 3.3). Continued movement would then raft the newly formed domes away from the central axis. The shape of the hummocks, and the lineated texture found within the hummocky zone in band C, is consistent with this interpretation. Larger hummocks, such as those observed in band B (Figure 10), could result from slower cracking and spreading. This would lead to a longer "dwell time" over the axis; hence larger hummocks could form. In addition, a longer time for the newly emplaced lithosphere to cool would allow larger hummocks to be supported. With the exception of those in Thynia Linea, hummocks are generally very closely spaced, precluding any obvious determination of spreading symmetry.

[50] An alternative explanation appears to be required for the origin of the hummocks comprising the Thynia Linea chevrons (Figure 15), which are different in character and distribution to the hummocks found within the hummocky zones on the other bands. One possible model for their formation is suggested by observations of the topography of the seafloor around the Reykjanes Ridge, part of the Mid-Atlantic Ridge, immediately south of Iceland. The Earth's seafloor in this area shows a series of southward pointing V-shaped topographic and gravity anomalies, with their apexes centered on regions of anomalously shallow depth at the ridge axis (Figure 21a) [*Vogt*, 1971; *Vogt and Avery*, 1974; *Owens et al.*, 1994]. The ridges may represent locally thickened crust due to (1) successive pulses of hotter than normal asthenosphere from the Icelandic hotspot, which have propagated south away from Iceland along the ridge axis [*Vogt*, 1971], or (2) thermal perturbations of the underlying asthenospheric mantle flowing south away from the hotspot [*White et al.*, 1995] (Figure 21b). On Europa the Thynia hummocks may have formed in an analogous fashion from pulses of ice or partial melt that were relatively warm with respect to the surrounding band material and propagated along the spreading axis. An alternative explanation was proposed by *Sullivan et al.* [1999b], who compared the morphology of Thynia Linea with patterns observed in magnetic anomaly data for the terrestrial Juan de Fuca ridge. The magnetic anomalies surrounding the Juan de Fuca ridge are interpreted to result from reorientation of ridge segments during spreading as a result of a southward propagating ridge spreading twice as rapidly as the existing ridge segment [*Wilson et al.*, 1984]. Similarities in the geometry of this data set with the distribution of the Thynia Linea hummocks led *Sullivan et al.* [1999b] to propose that spreading of the band had reoriented 10° clockwise from the original band axis immediately south of Delphi Flexus and ~7° clockwise ~20 km north of Delphi Flexus.

[51] In Europan band A, stereo imaging shows a narrow central depression containing the hummocky zone, which extends to either side of the axial trough. Beyond this broad depression where there is higher topography, lineaments are seen which are interpreted as

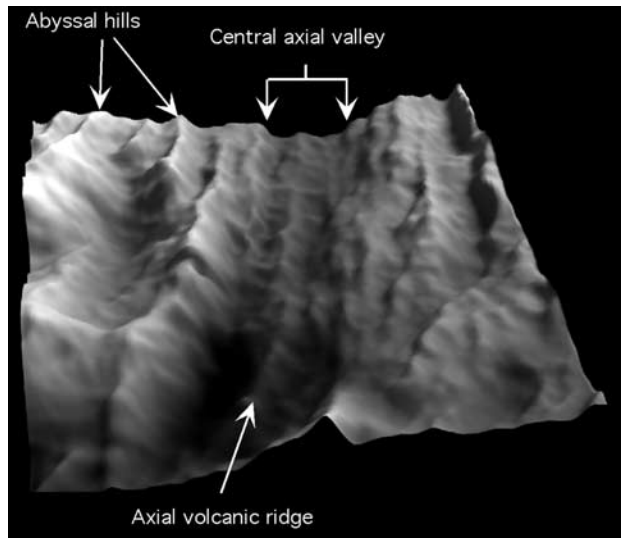


**Figure 20.** Seabeam bathymetry image of part of the Mid-Atlantic Ridge around 29°N. Data are projected into a perspective view looking along the central axial valley of the ridge. Width of valley floor is ~10 km.

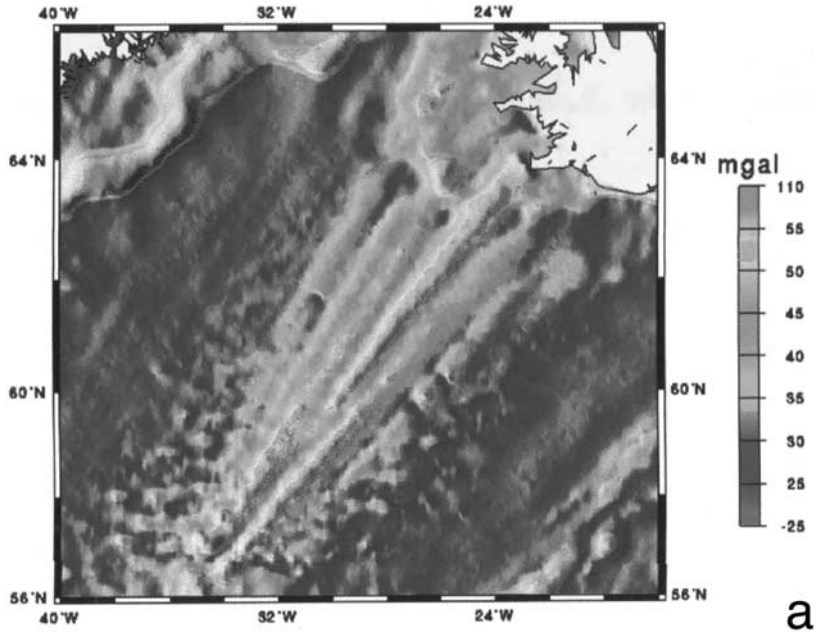


**Figure 21.** (a) Free-air gravity map of the Reykjanes Ridge showing location of V-shaped ridges caused by southwestward propagation of pulses of abnormally hot asthenosphere from the Icelandic plume (from *White et al.* [1995] with permission of the Geological Society of London). (b) Model of propagation of thermal heterogeneity southward along a spreading ridge [after *Vogt*, 1971].

faults or fractures. This sequence of units is directly analogous to a slow spreading terrestrial mid-ocean ridge, where the floor of the neovolcanic zone is bounded by faults marking the beginning of the topographically higher abyssal hills, which extend outward.

### 5.3. Faults and Fissures

[52] Vertical fractures (fissures) are ubiquitous along mid-ocean ridges (Figures 18 and 19). ''Abyssal hills'' are formed progressively on either side of the central axial rise or rift valley through normal faulting of the crust as it cools and moves away from the spreading axis. On the slow spreading Mid-Atlantic Ridge, fissures form most intensely between the distal edges of the neovolcanic zone and the inner walls of the rift valley and are probably formed through tensional failure during spreading [*MacDonald*, 1986] (Figure 22). Normal faults begin to form the abyssal hills at 1–5 km from the spreading axis and may continue forming up to 30 km off-axis at slow spreading ridges and 8–20 km off-axis at fast spreading ridges [*Shih*, 1980]. Faults may be up to 60 km in length along the slow spreading Mid-Atlantic Ridge and can have throws of up to 200 m [*MacDonald*, 1986]. At slow spreading ridges these faults are largely inward dipping, toward the axis, while at higher spreading rates the faults are likely to be oriented equally toward or away from the spreading axis, resulting in horst and graben structures [e.g., *MacDonald*, 1986] (Figure 18). At terrestrial spreading centers, to first order, slower spreading ridges exhibit larger, more widely spaced faults, while faster spreading ridges have smaller, more closely spaced faults [*Searle and Laughton*, 1981; *MacDonald*, 1982].

[53] Many of the features interpreted to be faults within Europan bands may be analogous to terrestrial abyssal hills. At high resolution, linear features interpreted to be fissures appear to ''slice up'' the background terrain (e.g., Figure 6c). These are similar in morphology to the numerous fractures found along some mid-ocean ridges as the lithosphere begins to cool and fracture (Figure 22). On Earth these fissures may later become reactivated as faults, forming the abyssal hills. Tilted fault blocks kilometers in length occur in both Europan band and terrestrial mid-ocean ridge environments (e.g., Figures 6, 12, and 19). Symmetry between faults on either side of the spreading axis is not so pronounced on Europan bands as at terrestrial spreading centers, perhaps because of differences in the timescale of band formation and overall band geometry. Terrestrial abyssal hills are responsible for the overall striated appearance of the regions surrounding mid-ocean ridges (Figure 19), and such tectonic features may also be responsible for imparting a similar appearance to Europan bands.

[54] The hummocky zone within band A is enclosed within a slight depression, apparently bounded by fault blocks at ~1 km on either side of the axis (Figure 4). *Edwards et al.* [1991] and *Carbotte and MacDonald* [1994] have shown that normal faulting is not common on fast spreading ridges within ±3 km of the axis, as the lithosphere is too thin and weak to support it. This explanation is likely applicable to Europan bands, in which the newly emplaced near-axis material is expected to be weak and would not yet have attained a sufficient thickness to support faults. In addition, *Chen and Morgan* [1990] note that the crust at fast spreading ridges is decoupled from extensional stresses by an axial magma chamber, further impeding near-axis faulting. In a spreading Europan band the apex of relatively warm, upwelling material would be expected to be located along the axis and might account for the absence of tensional features in the hummocky zone directly adjacent to the ridge axis.

### 5.4. Along-Strike Topographic Variations

[55] Variations exist in the along-strike segmentation of mid-ocean ridges and become more pronounced at lower spreading rates [e.g., *MacDonald et al.*, 1988; *Sempere et al.*, 1990]. Segmentation is defined at large scales (hundreds of kilometers) by transform faults and at small scales (0.5–3 km) by small offset spreading centers. Segmentation may be controlled by the distribution of partial melts within the lithosphere [*Toomey et al.*, 1990; *Gente et al.*, 1995], which feed magma chambers at discrete locations along the ridge, creating local depth anomalies. This hypothesis suggests that the magma supply is enhanced at segment centers but is starved at the discontinuities that bound the segments, for example, transform faults. This view is supported by

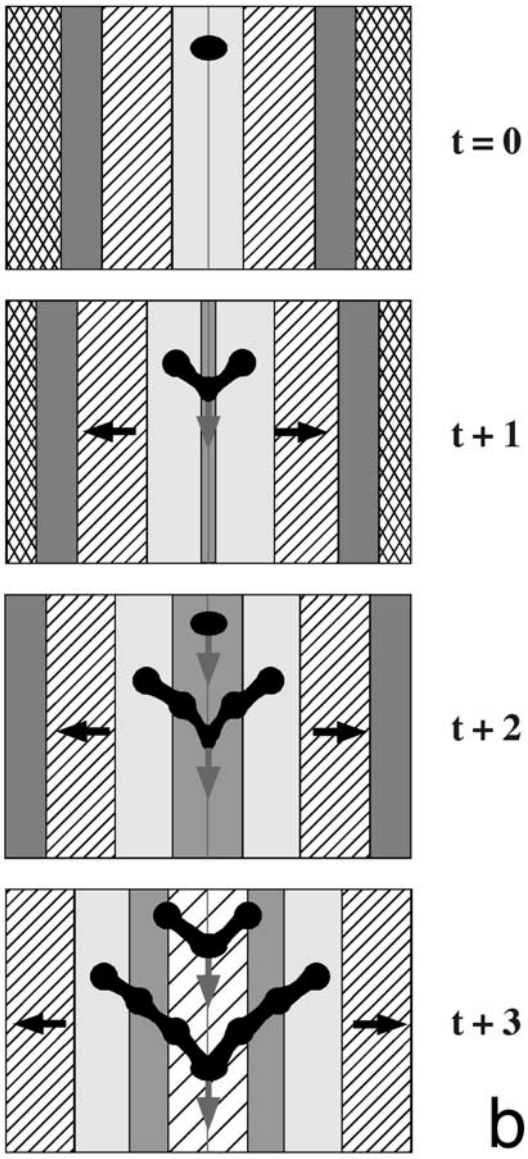


**Figure 21.** (continued)

axial volume estimates and studies of crustal magnetization (see *MacDonald* [1998] for review).

[56] Unlike terrestrial mid-ocean ridges, Europan bands do not appear to be segmented along their length. In fact, their boundaries and internal morphological features appear remarkably uniform along the length of each band. Since the scale of segmentation at terrestrial spreading centers becomes greater with increasing spreading rate, it appears that fast spreading ridges are underlain by an almost continuous narrow magma chamber, while slow spreading ridges may be underlain by discrete magma bodies [e.g., *Sinton and Detrick*, 1992]. The lack of segmentation along Europan bands may be evidence of a relatively homogenous asthenosphere, that is, one with no significant temperature or compositional variations.

[57] Oblique spreading is inferred at several places along terrestrial mid-ocean ridges, such as at the Reykjanes Ridge, and may be characterized by the disruption of volcanic and tectonic elements along the spreading axis into en echelon segments [e.g., *Searle and Laughton*, 1981], a more energetically favorable configuration. We have not observed any en echelon features along the axis of the Europan bands; neither are they broken up into en echelon segments. This implies that even if bands opened obliquely, the process of formation did not continue sufficiently long for the axis to reorient itself significantly. However, the suggestion by *Sullivan et al.* [1999b] that the axis of Thynia Linea has reoriented itself by a small amount may imply that this band formed at a slow enough rate to be affected by minor changes in the regional stress field. Most of the bands studied do show evidence of net oblique spreading, which may be the result of normal spreading interleaved with episodes of strike-slip offset.

### 5.5. Across-Axis Topographic Variations

[58] An axial high is common at fast spreading ocean ridges on Earth, with relief up to several hundred meters greater than that predicted by models of cooling and subsiding oceanic lithosphere [*Parsons and Sclater*, 1977]. This high relief is created beneath the axial spreading center by the buoyancy of upwelling magma and warm rock [*Sleep and Rosendahl*, 1979; *Madsen et al.*, 1984], and the thermal bulge decays with continued cooling. This axial high may be analogous to the enhanced topography observed over Europan band A, which is shown to stand 50–100 m above the surrounding plains (Figure 9). Band A may stand high because it is (1) thermally buoyant, (2) compositionally buoyant, or (3) a combination of the two. The temperature at the surface of Europa is only 100 K, while warm, convecting ice might be 260 K [*McKinnon*, 1999]. Simple buoyancy arguments imply that this temperature difference is sufficient to account for the topography inferred over the band. In addition, hydrated salt minerals have been identified on Europa [*McCord et al.*, 1999], and salt-rich material would be compositionally buoyant with respect to surrounding, salt-poor ice. Further work is needed to test these models.

[59] If the correlation between albedo and age on Europa is valid [*Pappalardo and Sullivan*, 1996; *Geissler et al.*, 1998; *Pappalardo et al.*, 1998c], then band A may be relatively young (it is certainly high in the stratigraphic column), and we may be seeing thermally buoyant topography that has not yet relaxed as a result of cooling. Stereo imaging over band B (Figure 11), which is lower in the stratigraphic column than band A, does not show the topographic elevation observed in band A, but instead shows a regional slope across the band. The lack of pronounced topography is consistent with the idea that band B is relatively old, and any thermal-induced topography may have relaxed.

### 5.6. Boundaries With Surrounding Terrain

[60] Earth's global tectonic system is a continuous assemblage of forming and subducting plates, constantly in motion. The cycle of plate formation and destruction is so vigorous that the majority of the seafloor is $\leq$200 Myr old. In contrast, Europan bands have formed in discrete, and probably short-lived, episodes, commonly

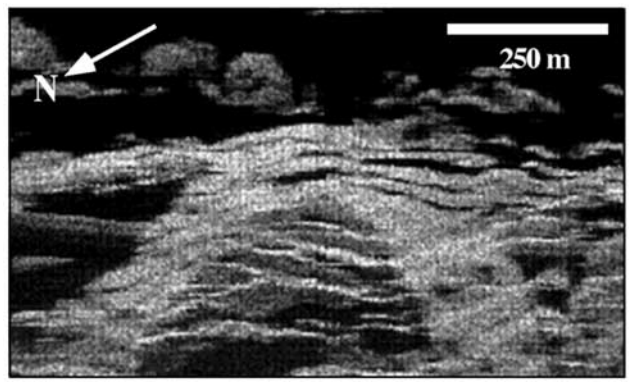


**Figure 22.** Image obtained using the British TOBI 30 kHz side-scan sonar system, showing fissures dissecting a seamount along the slow spreading Mid-Atlantic Ridge.

exploiting preexisting weaknesses, and then ceasing formation before they grow more than a few tens of kilometers wide.

[61] On Earth the East African Rift system appears to be a continuation of the ocean ridge system onto the continent. Terrestrial continental rifts such as this tend to be long and narrow, are bounded on one or both sides by master normal faults resulting in deep rift valleys, and are predominantly asymmetric [*Vening Meinesz*, 1950]. *Scholz and Contreras* [1998] model the initiation of the rift by the formation of a conjugate set of normal faults. One of these becomes the boundary fault system, while the other failed conjugate fault becomes locked against the first early in the rifting process, forming an asymmetric graben. Rift valleys may be several tens of kilometers wide, with several kilometers of displacement along their boundary fault system. Ultimately, the rift system may consist of a single graben or may contain several subparallel asymmetric graben.

[62] The fact that the margins of Europan bands can be reconstructed with virtually no loss of material strongly implies that they are initiated along tension fractures, rather than as fault-bounded graben that were subsequently flooded with cryovolcanic material [*Schenk and McKinnon*, 1989; *Golombek and Banerdt*, 1990]. Since mid-ocean ridge rift systems consist of graben, the process of rift initiation differs between Earth and Europa, a difference that may be attributable to the much lower strength and thickness of the Europan brittle lithosphere.

### 5.7. Driving Forces

[63] Two models have been proposed to account for the driving mechanism of plate tectonics (see *Bott* [1982] for comprehensive review): (1) a mantle drag mechanism, in which plate motion is envisaged to occur in response to the viscous drag exerted on the base of the lithosphere by the lateral motion of the tops of asthenospheric convection cells, and (2) an edge force mechanism, in which the plates move in response to forces applied to their edges as they lie atop the mantle convection system [*Forsyth and Uyeda*, 1975]. The edge force model is generally regarded as more acceptable than mantle drag for describing thermodynamic considerations and observations of past and present plate motions, and intraplate stress. In this model the main force acting on the edges of the separating plates is the ''ridge-push'' force, which derives from the buoyant upwelling of convecting mantle material beneath the zone of active rifting. At subduction zones the major force derives from the negative buoyancy of cold, descending plates, resulting in a ''slab-pull'' force. Potentially, the slab-pull force is four times greater than the ridge-push force, although much of it may be utilized in overcoming slab resistance [*Chappell and Tullis*, 1977].

[64] The slab-pull model is unlikely to be applicable to Europa, since no morphological features resembling subduction zones have yet been found. Although only parts of Europa's surface have been viewed at regional or high resolution, imaging has been sufficient to determine the presence of any features greater than a few kilometers in length [e.g., *Greeley et al.*, 2000, Plate 1, Table 1]. In addition, on Earth the margins of oceanic tectonic plates are subducted because they are cool and therefore relatively dense compared to the underlying asthenosphere. On Europa the uppermost shell is water ice, so even if it were underlain by a liquid water ocean, there would have to be a significant density difference for the shell to be subducted. Although there is evidence for low-density salts and other contaminants on Europa's surface [*McCord et al.*, 1999], it is not yet known whether these exist in sufficient quantities to affect the overall density of the lithosphere.

[65] Since Europan band formation has resulted from significant pulling apart of the lithosphere atop a mobile substrate, it seems likely that the driving force responsible for this process is convection as is the case on Earth [*Forsyth and Uyeda*, 1975] and that bands represent locally extended and thinned lithosphere in areas of relatively high heat flow. One model for the formation of Europa's ubiquitous double ridges proposes that they are the surface expression of buoyant ductile material that has risen along fractures to modify the surface [*Head et al.*, 1999a]. It is likely that bands form in a similar way and that they are the result of passive, rather than active, upwelling occurring after the brittle lithosphere has been fractured, although a detailed examination of this process is outside the scope of the present work.

## 6. Band Formation on Europa: Discussion

[66] One major question that has arisen with regard to the morphological features observed on Europa concerns whether the bands are formed from liquid water [*Greenberg et al.*, 1999; *Tufts et al.*, 2000] or relatively warm solid ice. The rise of water through a pure water-ice crust is precluded on the grounds of buoyancy, although the driving force to overcome this could be provided in one of several ways (see review by *Pappalardo et al.* [1999]). These are (1) pressurization of isolated liquid reservoirs by tidal stress or from ice crystallization—induced volume changes in the reservoir; (2) buoyancy-driven ascent if contaminants significantly modify the density of one phase with respect to the other [e.g., *Wilson and Head*, 1998]; (3) explosive cryovolcanism, which might be promoted by the presence of volatile compounds dissolved within the liquid water [*Crawford and Stevenson*, 1988]; and (4) pumping of water/ice mixtures to the surface by the initiation of fractures and their subsequent cyclic opening and closing as a result of diurnal tidal stresses [*Greenberg et al.*, 1998].

[67] On the basis of topography within the bands (such as axial troughs and linear ridges), and the observation that band A stands higher than its surroundings (Figure 9), we conclude that the material that formed the Europan ridges was ice that was thermally and/or compositionally buoyant compared to its surroundings. Warm ice would cool as soon as it reached the surface, forming a brittle lid, and the resulting thermal wave would propagate downward with time. Emplacement of relatively viscous material is consistent with the lack of any embayment seen adjacent to the band margins; no material appears to have extruded onto the surrounding plains, even when a band has no bounding ridges (e.g., bands C and E; Figures 12 and 15) or when a band stands higher than the surrounding plains (e.g., band A; Figures 4 and 9).

[68] On Earth the primary force driving the separation of plates at oceanic spreading centers is the subduction of plates at distant destructive margins. To date, no analogs to subduction zones have been found on Europa, and only a few compressional features have as yet been identified [*Prockter and Pappalardo*, 2000]. Some models have been proposed for the formation of the anti-Jovian rift zone (in which bands A and B are located) [*Schenk and McKinnon*, 1989]; these include (1) solid-state convection in a low-viscosity layer beneath the ice lithosphere; (2) external tidal forcing, ultimately resulting in a pivoting of the entire ice shell about its long axis; and (3) preferential strain accumulation in this region from the rest of the lithosphere. *Leith and McKinnon* [1996] have shown that the reorientation of the ice shell as a result of polar wander is unlikely, and consideration of other potential driving mechanisms for Europan band formation is outside the scope of this work. However, we hope that our observations may help to constrain future modeling efforts. The recent discovery of regional-scale folds on Europa [*Prockter and Pappalardo*, 2000] may shed light on how strain resulting from band formation may be accommodated, but the exact nature of the relationship between bands and folds (if any) is not yet clear. *Prockter and Pappalardo* [2000] have proposed a model for the recycling of the surface in which folds form as a result of band formation, and then, as folds relax isostatically, the underlying material ''flows'' back into the asthenosphere.

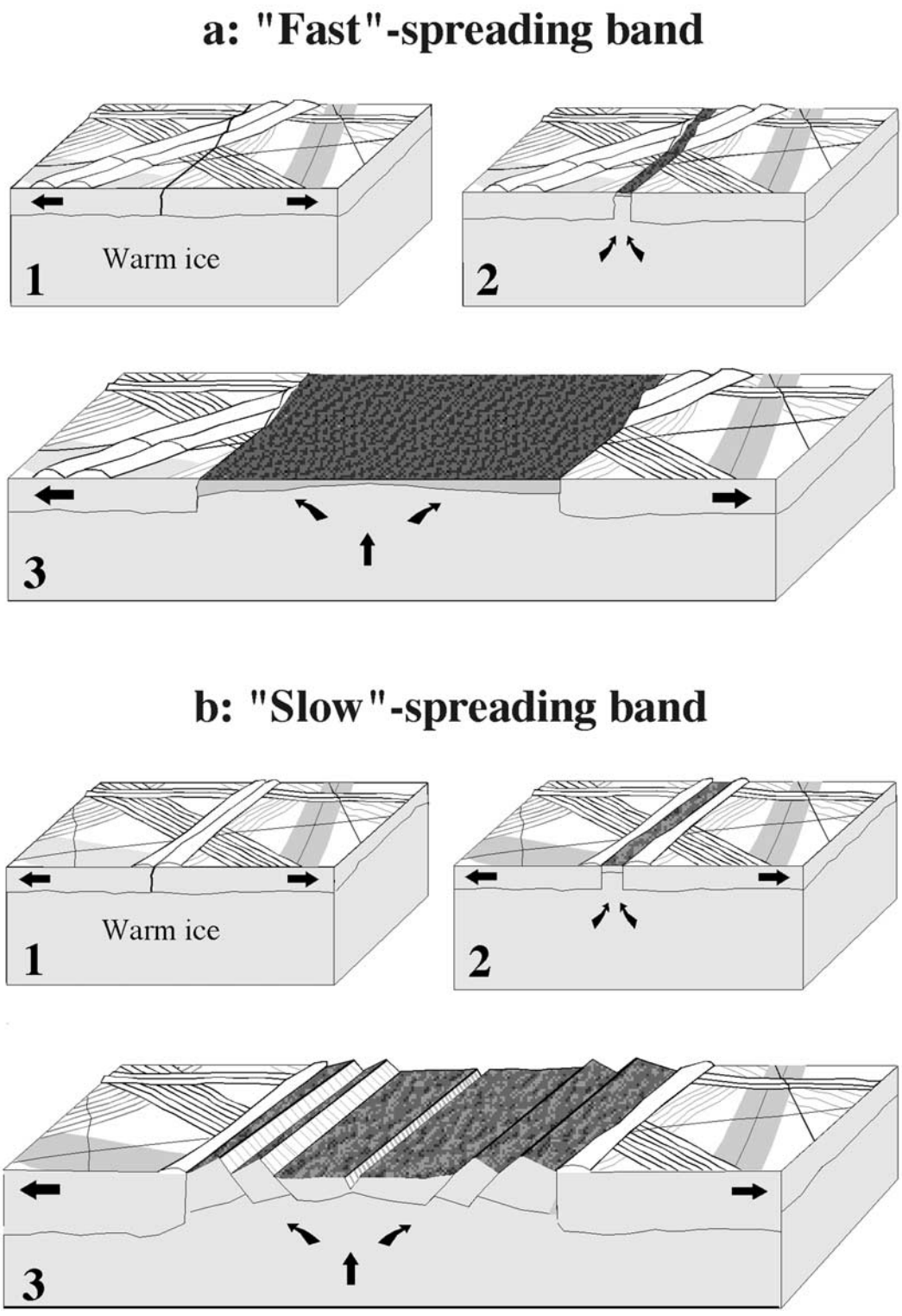


**Figure 23.** Spreading models for Europan bands. (a) "Fast" opening model. (1) Surface undergoes tension, which results in fracturing. (2) Warm ice wells up into gap, but spreading is sufficiently fast that a thick brittle shell does not have time to form. (3) Brittle layer is thin and weak and band topography is correspondingly subdued; band material has a uniform texture of small hummocks. No axial trough is apparent. (b) "Slow" opening model. (1) Surface is fractured or preexisting weakness is exploited, and (2) warm ice wells up into gap. Slow spreading results in significant thickening of brittle layer as new band material moves away from the emplacement axis. (3) With time, brittle layer reaches a sufficient thickness to fracture, resulting in enhanced topography. New material may pile up, forming pronounced hummocks, and a distinct axial trough is present.

[69] Some of the bands imaged by Galileo (including band A) have curvilinear margins, yet the innermost region of the band exhibits an axial trough and adjacent lineaments that are much straighter than the margins (e.g., band D; Figure 13). This implies that the opening axis of the bands straightened with time, as was suggested by *Sullivan et al.* [1998]. These workers suggest that straightening of lineaments toward the center of the band indicates intervals of inactivity long enough for structural adjustments to occur that affected the trend of succeeding spreading episodes. We have shown that some bands have experienced shear offset along their lengths. *Prockter et al.* [2000] examined Agenor Linea and found that horizontal shear, rather than extension, had played a significant role in the formation of this band. This has not been the case for the five bands studied here; extension appears to have been by far the dominant process, and shear does not appear to have significantly modified band morphology.

[70] Reconstruction of bands by the removal of interior materials may result in full closing of opposing band margins to form raised lineaments that closely resemble Europa's ubiquitous double ridges (Figures 7 and 14). This suggests two possible relationships between the formative mechanisms of bands and double ridges. One possibility is that band growth is a continuation of the ridge formation process, where ridges form through intrusion of subsurface solid-state material [*Head et al.*, 1999a]. As band formation progresses, the two halves of the initial double ridge recede from the central spreading axis as material continues to extrude to the surface. A second possibility is that band development is a fundamentally different process from ridge formation and occurs by exploiting preexisting axial troughs of double ridges. It is clear that in many instances these ridge troughs have provided locations for strike-slip motion between large lithospheric plates [e.g., *Hoppa et al.*, 1999b]. If the central troughs of double ridges are locations of weakness where movement between adjacent plates is localized, then it is likely these sites are places where plate separation (and associated band formation) would also occur. We favor this latter scenario, in which band and ridge formation are not related, on the basis of the following observations: (1) some bands have no bounding ridges; (2) bands may exploit more than one double ridge during their formation (e.g., band D, Figure 14b); and (3) the interiors of the bands studied have morphological features that bear little resemblance to the ridges bounding them.

[71] If the bands on Europa are analogous to terrestrial mid-ocean ridges (Table 2), and a similar mode of formation applies to both, then we can speculate on the cause of variations in morphology and topography among the Europan bands. If it is accepted that on Europa, as on terrestrial mid-ocean ridges, the effects of cooling outweigh the strain-rate dependence of the rifting process, then the variation in morphologies apparent in the Europan bands may be the result of differences in the rate of opening. One end-member of this process may be bands that lack prominent axial troughs and are composed of a uniformly small-scale hummocky textured material (e.g., bands C and E, Figures 12 and 15). These may have opened relatively rapidly, creating new lithosphere that did not thicken until well off-axis, resulting in somewhat subdued topography (Figure 23a). Europan bands that have a prominent axial trough, large hummocks, lineaments, and faults (e.g., bands A and B; Figures 4 and 10) may fall at the other end of the band spectrum. These bands may have opened relatively slowly, forming cooler, thicker lithosphere close to the axis, allowing significant topography to be supported (Figure 23b).

[72] It is recognized from sandbox analog and numerical models of tilt block style normal faulting that the spacing of tilted fault blocks is proportional to the local thickness of the faulted layer [*Vendeville et al.*, 1987; *Mandl*, 1987]. The precise relationship between fault spacing and brittle layer thickness is modeled to be a function of the shear softening behavior of the faulted material [*Witlox*, 1986]. While such a study for icy materials is beyond the scope of the present work, a valid rule of thumb is that the brittle layer thickness is similar to the observed fault spacing. We note that on Ganymede, a brittle lithosphere thickness of ~2 km has been independently estimated from the 5–10 km wavelengths of inferred extensional boudinage structures (i.e., the "grooves" inferred from Voyager images) [*Fink and Fletcher*, 1981; *Herrick and Stevenson*, 1990; *Collins et al.*, 1998; *Dombard and McKinnon*, 2001]. Using Fourier analysis, *Patel et al.* [1999a] find that fine-scale structures in these areas, which they interpret as tilt blocks, have a spacing ~2 km. Thus the two techniques appear to be consistent, suggesting that where fine-scale structures can be identified as tilt blocks, their spacing serves as a proxy for brittle layer thickness. Fourier analysis of lineaments in several Europan bands imaged at high resolution (the area shown in Figure 2) yields a dominant spacing of ~400 m [*Patel et al.*, 1999b], a value consistent with other estimates of brittle layer thickness derived for Europa (see *Pappalardo et al.* [1999] for review). For a nominal strain rate this thickness estimate implies a thermal gradient of 50–100 K/km. The mean spacing of inward dipping faults within part of the terrestrial East Pacific Rise (shown in Figure 19) is ~1.7 km [*Searle*, 1984], implying a much thicker terrestrial brittle lithosphere.

[73] We note that the most common wavelength of Europan bands is only ~1/4 of that measured for the inferred normal faulting induced component in Ganymede's grooved terrain. If the lineaments on Europa are tectonic, and considering that fault spacing is generally proportional to the thickness of the faulted layer, then the thickness of the Europan brittle lithosphere at the time of band fracturing may have been ~1/4 that of Ganymede's at the time of grooved terrain formation, i.e., $\ll$1 km for Europa. This implies that bands represent areas of locally extended and thinned lithosphere in regions of relatively high heat flow during their formation.

[74] The inferred thinness of the brittle layer is consistent with our suggestion, and that of *Pappalardo and Sullivan* [1996], that bands were a major resurfacing agent of Europa at least in the anti-Jovian hemisphere. Our observation that bands that are commonly disrupted by lenticulae (we have found no examples of lenticulae that are crosscut by bands) is consistent with the proposal by, for example, *Pappalardo et al.* [1998a] and *Prockter et al.* [1999] that Europa's lithosphere may have thickened with time, possibly as a result of the progressive freezing of a global ocean. This change in lithospheric thickness may have been accompanied by a corresponding change in the style of resurfacing from bands to lenticulae. This is in contrast to terrestrial seafloor spreading, which has been a relatively constant process throughout most of the Earth's history [e.g., *Bott*, 1982].

## 7. Summary

[75] Through detailed morphological studies, and comparison of Europan bands to terrestrial mid-ocean ridges, we are able to draw the following conclusions:

1. Bands have played a significant role in the resurfacing of Europa; in one region near the anti-Jovian point, ~60% of the ridged plains consists of bands.
2. During formation, bands may exploit preexisting weaknesses in the form of one or more double ridges.
3. Bands appear to have formed from the upwelling of thermally or compositionally buoyant ice, rather than liquid water.
4. Europan bands exhibit one or more of the following morphological elements: V-shaped axial trough, hummocky textures, fractures and/or tilted fault blocks, and bounding ridges.

5. Europan bands and terrestrial mid-ocean ridges have common characteristics, including broadly symmetrical spreading from a central axis that may include a trough, subcircular hummocks related to small-scale spreading processes, fractures and tilted fault blocks, and oblique opening.

6. A terrestrial seafloor-spreading analog appears appropriate for Europan bands. The internal morphological features of Europan bands may vary depending on the relative rate of band opening.

7. Europan bands are commonly postdated (but not predated) by lenticulae, implying that the style of resurfacing on Europa has changed with time.

[76] **Acknowledgments.** We wish to acknowledge our friend and colleague the late Randy Tufts, with whom we shared both wonder and bewilderment while trying to unravel the secrets of Europa. We will miss him. We wish to thank Patricio Figueredo for a thorough and useful review of this manuscript, Debbie Smith for permission to use the data shown in Figures 20 and 22, and Peter Neivert for creating Figure 20. R.T.P. acknowledges funding from the Jupiter System Data Analysis Program. L.P. gratefully thanks the Zonta International Organisation for the award of an Amelia Earhart fellowship.

## References

Anderson, J. D., G. Schubert, R. A. Jacobsen, E. L. Lau, W. B. Moore, and W. L. Sjogren, Europa's differentiated internal structure: Inferences from four Galileo encounters, *Science*, *276*, 1236–1239, 1998.

Ballard, R. D., E. Uchupi, D. K. Blackman, J. L. Cheminee, J. Francheteau, R. Hekinian, W. C. Schwab, and H. Siggurdsson, Geological mapping of the East Pacific Rise axis (10°19′–11°53′N) using Argo and ANGUS imaging systems, *Can. Mineral.*, *26*, 467–486, 1988.

Bonatti, E., and C. G. A. Harrison, Eruption styles of basalt in oceanic spreading ridges and seamounts: Effect of magma temperature and viscosity, *J. Geophys. Res.*, *93*, 2967–2980, 1988.

Bott, M. H. P., *The Interior of the Earth: Its Structure, Constitution and Evolution*, 2nd ed., Edward Arnold, London, 1982.

Carbotte, S. M., and K. C. MacDonald, Comparison of seafloor tectonic fabric at intermediate, fast, and super fast spreading ridges: Influence of spreading rate, plate motions, and ridge segmentation on fault patterns, *J. Geophys. Res.*, *99*, 13,609–13,631, 1994.

Carr, M. H., et al., Evidence for a subsurface ocean on Europa, *Nature*, *391*, 363–365, 1998.

Chadwick, W. W., Jr., and R. W. Embley, Graben formation associated with recent dike intrusions and volcanic eruptions on the mid-ocean ridge, *J. Geophys. Res.*, *103*, 9807–9825, 1998.

Chappell, W. M., and T. E. Tullis, Evaluation of the forces that drive plates, *J. Geophys. Res.*, *82*, 1967–1984, 1977.

Chen, Y., Oceanic crustal thickness versus spreading rate, *Geophys. Res. Lett.*, *19*, 953–956, 1992.

Chen, Y., and W. J. Morgan, Rift valley/no rift valley transition at mid-ocean ridges, *J. Geophys. Res.*, *95*, 17,571–17,581, 1990.

Cochran, J. R., J. A. Goff, A. Malinverno, D. J. Fornari, C. Keeley, and X. Wang, Morphology of a 'Superfast' mid-ocean ridge crest and flanks: The East Pacific Rise, 7°-9°S, *Mar. Geophys. Res.*, *15*, 65–75, 1993.

Collins, G. C., J. W. Head, and R. T. Pappalardo, The role of extensional instabilities in creating Ganymede grooved terrain: Insights from Galileo high resolution stereo imaging, *Geophys. Res. Lett.*, *25*, 233–236, 1998.

Collins, G. C., J. W. Head III, R. T. Pappalardo, and N. A. Spaun, Evaluation of models for the formation of chaotic terrain on Europa, *J. Geophys. Res.*, *105*, 1709–1716, 2000.

Crawford, G. D., and D. J. Stevenson, Gas-driven water volcanism and the resurfacing of Europa, *Icarus*, *73*, 66–79, 1988.

Dombard, A. J., and W. B. McKinnon, Formation of grooved terrain on Ganymede: Extensional instability mediated by cold, superplastic creep, *Icarus*, in press, 2001.

Edwards, M. H., D. J. Fornari, A. Malinverno, W. B. F. Ryan, and J. Madsen, The regional tectonic fabric of the East Pacific Rise from 12°50′N to 15°10′N, *J. Geophys. Res.*, *96*, 7995–8018, 1991.

Fagents, S. A., R. Greeley, R. J. Sullivan, R. T. Pappalardo, and L. M. Prockter, Cryomagmatic mechanisms for the formation of Rhadamanthys Linea, triple band margins, and other low albedo features on Europa, *Icarus*, *144*, 54–88, 2000.

Figueredo, P. H., and R. Greeley, Geologic mapping of the northern leading hemisphere of Europa from Galileo solid-state imaging data, *J. Geophys. Res.*, *105*, 22,629– 22,646, 2000.

Fink, J. H., and R. C. Fletcher, Variations in thickness of Ganymede's lithosphere determined by spacings of lineations, *Proc. Lunar Planet. Sci. Conf.*, *12th*, 277–278, 1981.

Fornari, D. J., Submarine lava tubes and channels, *Bull. Volcanol.*, *48*, 291–298, 1986.

Fornari, D. J., R. M. Haymon, M. R. Perfit, T. K. P. Gregg, and M. H. Edwards, Axial summit trough of the East Pacific Rise 9°–10°N: Geological characteristics and evolution of the axial zone on fast spreading mid-ocean ridges, *J. Geophys. Res.*, *103*(B5), 9827–9855, 1998.

Forsyth, D. W., Geophysical constraints on mantle flow and melt generation beneath mid-ocean ridges, in *Mantle Flow and Melt Generation Beneath Mid-ocean Ridges*, *Geophys. Monogr. Ser.*, vol. 71, edited by J. Phipps Morgan, D. K. Blackman, and J. M. Sinton, pp. 1–65, AGU, Washington, D. C., 1993.

Forsyth, D. W., and S. Uyeda, On the relative importance of driving forces of plate motion, *Geophys. J. R. Astron. Soc.*, *43*, 163–200, 1975.

Gaidos, E. J., and F. Nimmo, Tectonics and water on Europa, *Nature*, *405*, 637, 2000.

Geissler, P. E., et al., Evidence for nonsynchronous rotation of Europa, *Nature*, *391*, 368–371, 1998.

Gente, P., R. A. Pockalny, C. Durand, C. Deplus, M. Maia, G. Ceuleneer, C. Mével, M. Cannat, and C. Laverne, Characteristics and evolution of the segmentation of the Mid-Atlantic Ridge between 20°N and 24°N during the last 10 million years, *Earth Planet. Sci. Lett.*, *129*, 55–71, 1995.

Giese, B., J. Oberst, T. Roatsch, G. Neukum, J. W. Head, and R. T. Pappalardo, The local topography of Uruk Sulcus and Galileo Regio obtained from stereo images, *Icarus*, *135*, 303–316, 1998.

Golombek, M. P., and W. B. Banerdt, Constraints on the subsurface structure of Europa, *Icarus*, *83*, 441–452, 1990.

Greeley, R., et al., Europa: Initial Galileo geological observations, *Icarus*, *135*, 4–24, 1998.

Greeley, R., et al., Geologic mapping of Europa, *J. Geophys. Res.*, *105*, 22,559–22,578, 2000.

Greenberg, R., P. E. Geissler, G. Hoppa, B. R. Tufts, D. D. Durda, R. Pappalardo, J. W. Head, R. Greeley, R. Sullivan, and M. H. Carr, Tectonic processes on Europa: Tidal stresses, mechanical response, and visible features, *Icarus*, *135*, 64–78, 1998.

Haymon, R. M., The response of ridge crest hydrothermal systems to segmented, episodic magma supply, in *Tectonic, Magmatic, Hydrothermal and Biological Segmentation of Mid-Ocean Ridges,* edited by C. J. MacLeod, P. A. Taylor, and C. L. Walker, *Geol. Soc. Spec. Publ.*, *118*, 157–168, 1996.

Head, J. W., L. Wilson, and D. K. Smith, Mid-ocean ridge eruptive vent morphology and substructure: Evidence for dike widths, eruption rates, and evolution of eruptions and axial volcanic ridges, *J. Geophys. Res.*, *101*, 28,265–28,280, 1996.

Head, J. W., R. T. Pappalardo, R. Greeley, R. J. Sullivan, and the Galileo Imaging Team, Europan pits, spots, domes and ridges: Evidence for an origin through recent solid-state convection, *Geol. Soc. Am. Abstr. Programs*, *29*, A-312, 1997.

Head, J. W., N. D. Sherman, R. T. Pappalardo, R. Greeley, R. Sullivan, D. A. Senske, A. McEwen, and the Galileo Imaging Team, Geologic history of the E4 region of Europa: Implications for ridge formation, cryovolcanism, and chaos formation, *Lunar Planet. Sci*. [CD-ROM], *XXIX*, abstract 1412, 1998.

Head, J. W., R. T. Pappalardo, and R. Sullivan, Europa: Morphological characteristics of ridges and triple bands from Galileo data (E4 and E6) and assessment of a linear diapirism model, *J. Geophys. Res.*, *104*, 24,223–24,236, 1999a.

Head, J. W., R. T. Pappalardo, L. M. Prockter, N. A. Spaun, G. C. Collins, R. Greeley, J. Klemaszewski, R. Sullivan, C. Chapman, and the Galileo SSI Team, Europa: Recent geological history from Galileo observations, *Lunar Planet. Sci*. [CD-ROM], *XXX*, abstract 1404, 1999b.

Herrick, D. L., and D. J. Stevenson, Extensional and compressional instabilities in icy satellite lithospheres, *Icarus*, *85*, 191–204, 1990.

Hoppa, G. V., B. R. Tufts, R. Greenberg, and P. E. Geissler, Formation of cycloidal features on Europa, *Science*, *285*, 1899–1902, 1999a.

Hoppa, G. V., B. R. Tufts, R. Greenberg, and P. E. Geissler, Strike-slip faults on Europa: Global shear patterns driven by tidal stress, *Icarus*, *141*, 287–298, 1999b.

Jacoby, W. R., Morphology of the Reykjanes Ridge crest near 62°N, *J. Geophys.*, *47*, 81–85, 1980.

Lachenbruch, A. H., A simple mechanical model for oceanic spreading centers, *J. Geophys. Res.*, *78*, 3395–3417, 1973.

Leith, A. C., and W. B. McKinnon, Is there evidence for polar wander on Europa?, *Icarus*, *120*, 387–398, 1996.

Lonsdale, P., Structural geomorphology of a fast spreading rise crest: The East Pacific Rise near 3°25′s, *Mar. Geophys. Res.*, *3*, 251–293, 1977.

MacDonald, K. C., Mid-ocean ridges: Fine scale tectonic, volcanic, and hydrothermal processes within the plate boundary zone, *Annu. Rev. Earth Planet. Sci.*, *10*, 155–190, 1982.

MacDonald, K. C., The crest of the Mid-Atlantic Ridge: Models for crustal generation processes and tectonics, in *The Western North Atlantic Region,* edited by P. Vogt and B. Tucholke, pp. 51–68, Geol. Soc. of Am., Boulder, Colo., 1986.

MacDonald, K. C., Linkages between faulting, volcanism, hydrothermal activity and segmentation on fast spreading centers, in *Faulting and Magmatism at Mid-Ocean Ridges*, *Geophys. Monogr. Ser.*, vol. 106, edited by W. R. Buck et al., pp. 27–58, AGU, Washington, D. C., 1998.

MacDonald, K. C., and P. J. Fox, The axial summit graben and cross-sectional shape of the East Pacific Rise as indicators of axial magma chambers and recent volcanic eruptions, *Earth Planet. Sci. Lett.*, *88*, 119–131, 1988.

MacDonald, K. C., P. J. Fox, L. J. Perram, M. F. Eisen, R. M. Haymon, S. P. Miller, S. M. Carbotte, M.-H. Cormier, and A. N. Shor, A new view of the mid-ocean ridge from the behavior of ridge-axis discontinuities, *Nature*, *335*, 217–225, 1988.

Madsen, J. A., D. W. Forsyth, and R. S. Detrick, A new isostatic model for the East Pacific Crest, *J. Geophys. Res.*, *89*, 9997–10,015, 1984.

Malinverno, A., A quantitative study of axial topography of the Mid-Atlantic Ridge, *J. Geophys. Res.*, *95*, 2645–2660, 1990.

Mandl, G., Tectonic deformation by rotating parallel faults: The bookshelf mechanism, *Tectonophysics*, *141*, 277–316, 1987.

McCord, T. B., et al., Hydrated salt minerals on Europa's surface from the Galileo near-infrared mapping spectrometer (NIMS) investigation, *J. Geophys. Res.*, *104*, 11,827–11,851, 1999.

McKinnon, W. B., Convective instability in Europa's floating ice shell, *Geophys. Res. Lett.*, *26*, 951–954, 1999.

Morgan, J. P., and Y. J. Chen, Dependence of ridge-axis morphology on magma supply and spreading rate, *Nature*, *364*, 706–708, 1993.

Owens, R., B. Parsons, L. Parson, and B. Murton, The Reykjanes Ridge: Dynamics of ridge-hotspot interaction from satellite gravity data (abstract), *Eos Trans. AGU*, *75*(16), Spring Meet. Suppl., 335, 1994.

Pappalardo, R. T., and R. J. Sullivan, Evidence for separation across a gray band on Europa, *Icarus*, *123*, 557–567, 1996.

Pappalardo, R. T., et al., Geological evidence for solid-state convection in Europa's ice shell, *Nature*, *391*, 365–368, 1998a.

Pappalardo, R. T., N. D. Sherman, J. W. Head, G. C. Collins, R. Greeley, J. Klemaszewski, R. Sullivan, C. B. Phillips, A. S. McEwen, and the Galileo Imaging Team, Distribution of mottled terrain on Europa: A possible link to nonsynchronous rotation stresses, *Lunar Planet. Sci.* [CD-ROM], *XXIX*, abstract 1923, 1998b.

Pappalardo, R. T., J. Spencer, P. E. Geissler, L. M. Prockter, G. C. Collins, J. W. Head, P. Helfenstein, and the Galileo Imaging Team, What controls the albedo patterns on Europa?, *Eos Trans. AGU.*, *79*(17), Spring Meet. Suppl., S198–S199, 1998c.

Pappalardo, R. T., et al., Does Europa have a subsurface ocean? Evaluation of the geological evidence, *J. Geophys. Res.*, *104*, 24,015–24,056, 1999.

Parson, L. M., et al., En echelon axial volcanic ridges at the Reykjanes Ridge: A life cycle of volcanism and tectonics, *Earth Planet. Sci. Lett.*, *117*, 73–87, 1993.

Parsons, B., and J. G. Sclater, An analysis of the variation of ocean floor bathymetry and heat flow with age, *J. Geophys. Res.*, *82*, 803–827, 1977.

Patel, J. G., R. T. Pappalardo, J. W. Head, G. C. Collins, H. Heisinger, and J. Sun, Topographic wavelengths of Ganymede groove lanes from Fourier analysis of Galileo images, *J. Geophys. Res.*, *104*, 24,057–24,074, 1999a.

Patel, J. G., R. T. Pappalardo, L. M. Prockter, G. C. Collins, J. W. Head, and the Galileo SSI Team, Morphology of ridge and trough terrain on Europa: Fourier analysis and comparison to Ganymede, *Eos Trans AGU.*, *80*(17) Spring Meet. Suppl., S210, 1999b.

Perfit, M. R., and W. W. Chadwick, Magmatism at mid-ocean ridges: Constraints from volcanological and geochemical investigations, in *Faulting and Magmatism at Mid-Ocean Ridges*, *Geophys. Monogr. Ser.*, vol. 106, edited by W. R. Buck et al., pp. 59–116, AGU, Washington, D. C., 1998.

Prockter, L. M., and R. T. Pappalardo, Folds on Europa: Implications for crustal cycling and accommodation of extension, *Science*, *289*, 941–943, 2000.

Prockter, L. M., R. Sullivan, J. W. Head, R. T. Pappalardo, A. Antman, and the Galileo SSI Team, Wedges and bands on Europa as imaged by Galileo: Stratigraphy, morphology and evolution, *Eos Trans AGU*, *79*, P22B-10, 1998.

Prockter, L. M., A. M. Antman, R. T. Pappalardo, J. W. Head, and G. C. Collins, Europa: Stratigraphy and geological history of the anti-Jovian region from Galileo E14 solid-state imaging data, *J. Geophys. Res.*, *104*, 16,531–16,540, 1999.

Prockter, L. M., R. T. Pappalardo, and J. W. Head, Strike-slip duplexing on Jupiter's icy moon Europa, *J. Geophys. Res.*, *105*, 9483–9488, 2000.

Scheirer, D. S., and K. C. MacDonald, Near-axis seamounts on the flanks of the East Pacific Rise, 8°N to 17°N, *J. Geophys. Res.*, *100*, 2239–2259, 1995.

Schenk, P. M., and W. B. McKinnon, Fault offsets and lateral crustal movement on Europa: Evidence for a mobile ice shell, *Icarus*, *79*, 75–100, 1989.

Scholz, C. H., and J. C. Contreras, Mechanics of continental rift architecture, *Geology*, *26*, 967–970, 1998.

Searle, R. C., Gloria survey of the East Pacific Rise near 3.5°S: Tectonic and volcanic characteristics of a fast-spreading mid-ocean rise, *Tectonophysics*, *101*, 319–344, 1984.

Searle, R. C., and A. S. Laughton, Fine-scale sonar study of tectonics and volcanism on the Reykjanes Ridge, *Oceanol. Acta*, *4*, suppl., 5–13, 1981.

Sempere, J.-C., G. M. Purdy, and H. Schouten, Segmentation of the Mid-Atlantic Ridge between 24°N and 30°40′N, *Nature*, *344*, 427–429, 1990.

Shih, J. S. F., The nature and origin of fine-scale seafloor relief, Ph.D. thesis, 222 pp., Mass. Inst. of Technol, Cambridge, Mass., 1980.

Sinton, J. M., and R. S. Detrick, Mid-ocean ridge magma chambers, *J. Geophys. Res.*, *97*, 197–216, 1992.

Sleep, N. H., Sensitivity of heat flow and gravity to the mechanism of seafloor spreading, *J. Geophys. Res.*, *74*, 542–549, 1969.

Sleep, N. H., and B. R. Rosendahl, Topography and tectonics of mid-ocean ridge axes, *J. Geophys. Res.*, *84*, 6831–6839, 1979.

Small, C., Global systematics of mid-ocean ridge morphology, in *Faulting and Magmatism at Mid-Ocean Ridges*, edited by W. R. Buck et al., *Geophys. Monogr. Ser.*, vol. 106, pp. 1–26, AGU, Washington, D. C., 1998.

Smith, B. A., and the Voyager Imaging Team, The Galilean satellites of Jupiter: Voyager 2 imaging science results, *Science*, *206*, 951–972, 1979.

Smith, D. K., and J. R. Cann, The role of seamount volcanism in crustal construction at the Mid-Atlantic Ridge (23°–30°N), *J. Geophys. Res.*, *97*, 1645–1658, 1992.

Smith, D. K., S. E. Humphris, and W. B. Bryan, A comparison of volcanic edifices at the Reykjanes Ridge and the Mid-Atlantic Ridge at 24°–30°N, *J. Geophys. Res.*, *100*, 22,485–22,498, 1995.

Spaun, N. A., J. W. Head III, L. M. Prockter, G. C. Collins, R. T. Pappalardo, and the Galileo Imaging Team, Chaos and microchaos: Mapping, unit descriptions, and origins, *Eos Trans AGU*, *79*(45), Fall Meet. Suppl., F540, 1998.

Spencer, J. R., L. Prockter, R. Pappalardo, J. Head, J. Moore, and the Galileo SSI Team, Local volatile migration on Ganymede: Galileo SSI images, PPR radiometry and theoretical considerations, *Lunar Planet. Sci.* [CD-ROM], *XXIX*, abstract 1149, 1998.

Squyres, S. W., R. T. Reynolds, P. Cassen, and S. J. Peale, Liquid water and active resurfacing on Europa, *Nature*, *301*, 225–226, 1983.

Stevenson, D. J., Limits on the variation of thickness of Europa's shell, *Lunar Planet. Sci*., [CD-ROM], *XXXI*, abstract 1506, 2000.

Sullivan, R., et al., Episodic plate separation and fracture infill on the surface of Europa, *Nature*, *391*, 371–373, 1998.

Sullivan, R., R. Pappalardo, L. Prockter, J. Klemaszewski, and the Galileo Imaging Team, Europa: High resolution views of spreading at Thynia Linea, *Lunar Planet. Sci*. [CD-ROM], *XXX*, abstract 2059, 1999a.

Sullivan, R., J. Moore, and R. Pappalardo, Mass-wasting and slope evolution on Europa, *Lunar Planet. Sci*. [CD-ROM], *XXX*, abstract 1747, 1999b.

Tapponier, P., and J. Francheteau, Necking of the lithosphere and the mechanics of slowly accreting plate boundaries, *J. Geophys. Res.*, *83*, 3955–3970, 1978.

Toomey, D. R., G. M. Purdy, S. C. Solomon, and W. S. D. Wilcock, The three dimensional seismic velocity structure of the East Pacific Rise near latitude 930′N, *Nature*, *347*, 639–645, 1990.

Tufts, B. R., R. Greenberg, R. Sullivan, and R. Pappalardo, and the Galileo Imaging Team, Reconstruction of Europan terrain in the Galileo C3 "Wedges" image and its geological implications (abstract), *Proc. Lunar Planet. Sci. Conf.*, *27th*, 1455–1456, 1997.

Tufts, B. R., R. Greenberg, G. Hoppa, and P. Geissler, Astypalaea Linea, a large-scale strike-slip fault on Europa, *Icarus*, *141*, 53–64, 1999.

Tufts, B. R., R. Greenberg, G. Hoppa, and P. Geissler, Lithospheric dilation on Europa, *Icarus*, *146*, 75–97, 2000.

Vendeville, B., P. R. Cobbold, P. Davy. J. P. Brun, and P. Choukroune, Physical models of extensional tectonics at various scales, in *Continental Extensional Tectonics*, edited by M. P. Coward et al. *Spec. Publ. Geol. Soc. Am.*, *28*, 95–107, 1987.

Vening Meinesz, F. A., Les graben africains resultant de compression ou de tension dans la croute terrestre?, *Inst. R. Coll. Belge Bull.*, *21*, 539–552, 1950.

Vogt, P. R., Asthenosphere motion recorded by the ocean floor south of Iceland, *Earth Planet. Sci. Lett.*, *13*, 153–160, 1971.

Vogt, P. R., and O. E. Avery, Detailed magnetic surveys in the northeast Atlantic and the Labrador Sea, *J. Geophys. Res.*, *79*, 363–389, 1974.

White, R. S., J. W. Bown, and J. R. Smallwood, The temperature of the Iceland plume and origin of outward-propagating V-shaped ridges, *J. Geol. Soc. London*, *152*, 1039–1045, 1995.

Wilson, D. S., R. N. Hey, and C. Nishimura, Propagation as a mechanism for reorientation of the Juan deFuca Ridge, *J. Geophys. Res.*, *89*, 9215–9225, 1984.

Wilson, L., and J. W. Head, Europa cryovolcanism: Ascent and eruption of magma and its role in resurfacing, *Lunar Planet. Sci*. [CD-ROM], *XXIX*, abstract 1138, 1998.

Witlox, H. W. M., Finite element simulation of basal extensional faulting within a sediment overburden, paper presented at First European Conference on Numerical Methods in Geomechanics, Stuttgart, Germany, 16–18 Sept. 1986.

A. E. Clifton, Nordic Volcanological Institute, Grensasvegur 50, 104 Reykjavik, Iceland.

B. Giese, G. Neukum, and R. Wagner, Institute of Planetary Exploration, DLR, Berlin D-12489, Germany.

J. W. Head III and R. T. Pappalardo, Department of Geological Sciences, Box 1846, Brown University, Providence, RI 02912, USA.

L. M. Prockter, Applied Physics Laboratory, MS 7-366, 11100 Johns Hopkins Road, Laurel, MD 20723, USA. (Louise.Prockter@jhuapl.edu)

R. J. Sullivan, Center for Radiophysics and Space Research, 308 Space Sciences, Cornell University, Ithaca, New York 14853, USA.

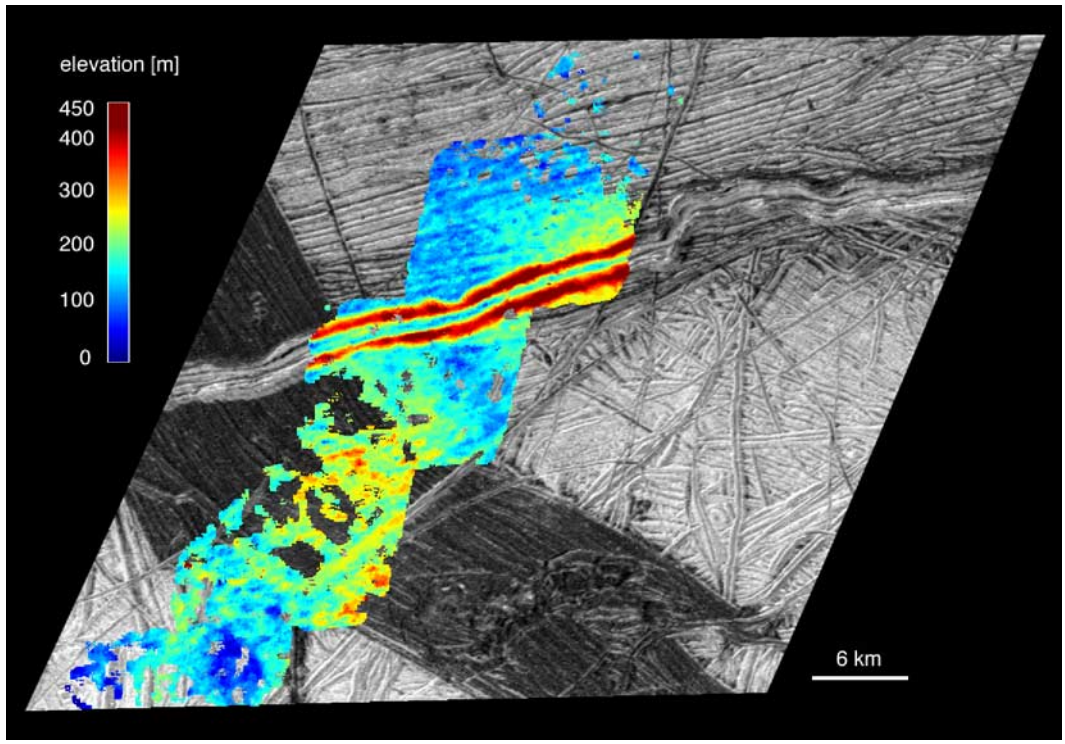


**Figure 9.** Digital terrain model of band A showing height differences of up to 100 m between the band and the surrounding plains.

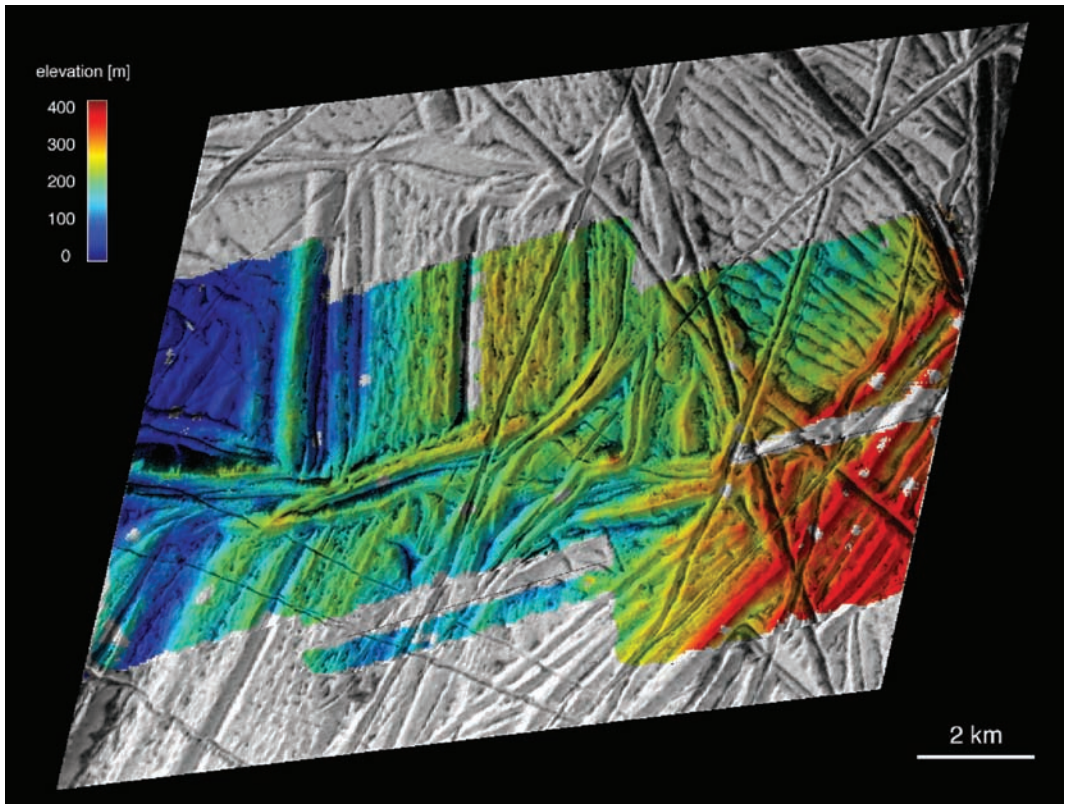


**Figure 11.** Digital terrain model of band B showing no distinct height variations across the band but a regional slope rising from west to east.